

Separation of S -wave pseudoscalar and pseudovector amplitudes in $\pi^- p_{\uparrow} \rightarrow \pi^+ \pi^- n$ reaction on polarized target

R. Kamiński, L. Leśniak and K. Rybicki
Henryk Niewodniczański Institute of Nuclear Physics,
PL 31-342 Kraków, Poland

June 19, 2018

Abstract

A new analysis of S -wave production amplitudes for the reaction $\pi^- p_{\uparrow} \rightarrow \pi^+ \pi^- n$ on a transversely polarized target is performed. It is based on the results obtained by the CERN–Cracow–Munich collaboration in the $\pi\pi$ energy range from 600 MeV to 1600 MeV at 17.2 GeV/ c π^- momentum. Energy-independent separation of the S -wave pseudoscalar amplitude (π exchange) from the pseudovector amplitude (a_1 exchange) is carried out using assumptions much weaker than those in all previous analyses. We show that, especially around 1000 MeV and around 1500 MeV, the a_1 exchange amplitude cannot be neglected. The scalar–isoscalar $\pi\pi$ phase shifts are calculated using fairly weak assumptions.

Below the $K\bar{K}$ threshold we find two solutions for the $\pi - \pi$ phase shifts, for which the phases increase slower with the effective $\pi - \pi$ mass than the P-wave phases. Both solutions are consistent with a broad $f_0(500)$ but only one is similar to the well-known "down" solution. We find also the third solution (with a somewhat puzzling behavior of inelasticity) which exhibits a narrow $f_0(750)$ claimed by Svec. All the solutions undergo a rapid change at the $K\bar{K}$ threshold. Above 1420 MeV the phase shifts increase with energy faster than those obtained without the polarized-target data. This phase behavior as well as an increase of the modulus of the a_1 -exchange amplitude can be due to the presence of the $f_0(1500)$.

1 Introduction

Study of scalar mesons is one of the central points of light quark spectroscopy. In addition to ordinary $q\bar{q}$ mesons, some $K\bar{K}$ bound states [1, 2] and lowest-lying glueballs are expected as well [3, 4, 5, 6, 7]. Unfortunately, the experimental situation is still far from being clear [8, 9, 10, 11]. In the effective mass region above 1000 MeV, a rich spectrum of scalar mesons has been recently proposed and discussed in many experimental [12, 13] and theoretical [6, 7, 14] papers. Generally, the proposed scalar states have a coupling to the $\pi\pi$ channel strong enough to manifest themselves through energy dependence of the $\pi\pi$ interaction amplitudes. In the past few years scalar resonance $f_0(1500)$ related to a hypothetical lowest lying glueball state was announced [3, 4, 5, 15]. Thus, a study of the $\pi\pi$ interaction near 1500 MeV is important also in this context. Below 1000 MeV the status of scalar mesons is also unclear since the existence of a broad σ or $f_0(750)$ meson still remains an open question [2, 16, 17, 19].

One of the main sources of information on the production of scalar states is the $\pi\pi$ partial wave analysis (PWA) yielding the S -wave. It should be stressed that study of S -wave objects *does require* the partial wave analysis to "subtract" contributions of leading mesons $\rho(770)$, $f_2(1270)$ and $\rho_3(1690)$ which dominate the total cross section. Virtually all PWA's were based on the old CERN-Munich experiment [20] which supplied 3×10^5 events of the reaction

$$\pi^- p \rightarrow \pi^+ \pi^- n \quad (1)$$

at 17.2 GeV/c. The number of observables provided by such experiment is much smaller than the number of real parameters needed to describe the partial waves. Consequently, the dominance of pseudoscalar exchange, equivalent to the absence of pseudovector exchange and several other physical assumptions have been made in previous studies [20]–[25].

In this paper we use results of PWA performed in the energy range from 600 MeV to 1600 MeV (in 20 MeV bins) obtained with the help of the polarized target experiment. This experiment, performed 20 years ago by the CERN-Cracow-Munich collaboration, provided 1.2×10^6 events of the reaction

$$\pi^- p_{\uparrow} \rightarrow \pi^+ \pi^- n \quad (2)$$

also at 17.2 GeV/c [26]. Combination of results of both experiments yields a number of observables sufficient for performing a quasi-complete and energy independent PWA without any model assumptions. This analysis is only quasi-complete because of an unknown phase between two sets of transversity

amplitudes. Nevertheless, intensities of partial waves could be determined in a completely model-independent way. This removed ambiguities appearing in earlier studies, except for the old "up-down" ambiguity [21]. The "up" solution contains an S -wave resonance just under the $\rho(770)$ and of similar width, while the "down" S -wave modulus stays high and nearly constant all the way to the $f_0(980)$. It was only Svec[16, 17] who argued persistently in favour of the "up" solution, using both the 17.2 GeV data as well as data on the reaction $\pi^+p_{\uparrow} \rightarrow \pi^+\pi^-p$ at 5.85 and 11.98 GeV/c. However, general belief (see e.g. [27], [28]) was that the "up-down" ambiguity had been resolved definitely in favour of the "down" solution. We disagree with this belief since all the previous studies of the *full* 17.2 GeV/c data were consistent with both the "up" and "down" solutions. The same is true for the present analysis. We stress this point because the mini-reviews in the last RPP editions (see e.g. Ref. [29]) contained the sentence "BECKER 79B [30] excluded a narrow resonance behaviour for δ_0^0 ..." , contrary to what is stated explicitly in another paper of the same collaboration (see Sect. 6 of [26]): "...our results do not give a clear answer to this ambiguity...".

In this paper we make another step in the analysis of 17.2 GeV/c data attempting to bridge two sets of transversity amplitudes. The phase of each S -wave transversity amplitude is fixed by requiring the phase of the leading P , D , F -waves to follow roughly the phase of the Breit-Wigner amplitudes of the $\rho(770)$, $f_2(1270)$ and $\rho_3(1690)$ resonances in the low, medium and high mass region respectively. This fairly reasonable assumption allows us to separate explicitly for the first time the pseudoscalar and pseudovector amplitudes in the S -wave.

In Sect. 2 we present mathematical formalism needed to separate the one-pion and a_1 exchange amplitudes for the reaction on a polarized target. Section 3 contains a short description of the PWA done by the CERN-Cracow-Munich collaboration for reaction (2). In Sect. 4 we present our analysis yielding pseudoscalar and pseudovector reaction amplitudes. Further on, from the pseudoscalar amplitude we extract the $I = 0$, S -wave amplitude describing the $\pi\pi$ elastic scattering amplitude. Our results are discussed in Sect. 4 and summarized in Sect. 5.

2 Amplitudes describing pion pair production in the $I = 0$, S -wave

a) Separation of pseudoscalar and pseudovector exchange amplitudes

Let us denote by f_0 a system of two pions in a relative S -wave isospin

0 state. Transition amplitude for the f_0 production process $\pi^- p \rightarrow f_0 n$ can be written as the following matrix element

$$T_{s_p s_n} = \langle u_{p_2}^{s_n} | A \gamma_5 + \frac{1}{2} B \gamma_5 \gamma_\mu (p_\pi + p_f)^\mu | u_{p_1}^{s_p} \rangle, \quad (3)$$

where p_1, p_2, p_π and p_f are proton, neutron, incoming pion, and final f_0 four-momenta, s_p and s_n are proton and neutron spin projections, $u_{p_1}^{s_p}$ and $u_{p_2}^{s_n}$ are the corresponding four-spinors, A and B are functions of the Mandelstam variables $s = (p_1 + p_\pi)^2$ and $t = (p_1 - p_2)^2$ at fixed f_0 mass $m_{\pi\pi}$. Part A of the amplitude corresponds to the pseudoscalar (or one pion) exchange while part B describes the pseudovector exchange which we shall briefly call a_1 exchange since we expect that the a_1 meson exchange amplitude constitutes its major contribution. Functions A and B have to be determined from experiment. Using s-channel helicity amplitudes in the c.m. $\pi^- p$ system one can derive the following two independent amplitudes [21]:

$$H_{++} \equiv T_{\frac{1}{2}\frac{1}{2}} = -T_{-\frac{1}{2}-\frac{1}{2}}, \quad (4)$$

$$H_{+-} \equiv T_{\frac{1}{2}-\frac{1}{2}} = T_{-\frac{1}{2}\frac{1}{2}}, \quad (5)$$

$$H_{++} = \left(\frac{A}{2M} \sqrt{-t_{min}} - \frac{B}{2} \frac{m_f^2 - m_\pi^2}{\sqrt{-t_{min}}} \right) \cos \frac{\Theta_s}{2}, \quad (6)$$

$$H_{+-} = \left(-\frac{A}{2M} \sqrt{-t_{max}} + \frac{B}{2} \frac{m_f^2 - m_\pi^2}{\sqrt{-t_{max}}} \right) \sin \frac{\Theta_s}{2}. \quad (7)$$

In (5-6) Θ_s is the neutron scattering angle (with respect to proton direction), M and m_π are nucleon (proton and neutron average) and pion masses, t_{min} and t_{max} are expressed by momenta p_1, p_2 and the corresponding c.m. energies E_1, E_2 :

$$t_{min} = 2(M^2 + p_1 p_2 - E_1 E_2), \quad (8)$$

$$t_{max} = 2(M^2 - p_1 p_2 - E_1 E_2). \quad (9)$$

The scattering angle is related to the four-momentum transfer squared t :

$$\sin \frac{\Theta_s}{2} = \sqrt{\frac{t_{min} - t}{t_{min} - t_{max}}}. \quad (10)$$

In this paper we use two amplitudes g and h , closely related to H_{++} and H_{+-} , adequate for describing f_0 production on a transversely polarized target:

$$g \equiv \langle n \downarrow | T | p \uparrow \rangle = (H_{+-} - i H_{++}) \exp\left(\frac{1}{2} i \Theta_s\right), \quad (11)$$

$$h \equiv \langle n \uparrow | T | p \downarrow \rangle = (H_{+-} + i H_{++}) \exp\left(-\frac{1}{2} i \Theta_s\right). \quad (12)$$

In this case, nucleon spin is quantized along the vector $\mathbf{n} = \mathbf{p}_1 \times \mathbf{p}_2$ normal to the production plane (in (11) and (12), arrows \uparrow and \downarrow denote spin projections parallel or antiparallel to \mathbf{n}). It can be shown that the remaining two matrix elements vanish:

$$\langle n \uparrow | T | p \uparrow \rangle = \langle n \downarrow | T | p \downarrow \rangle = 0. \quad (13)$$

Separation of invariant amplitudes A and B for the reaction $\pi^- p \rightarrow f_0 n$ for *fixed* values of t and $m_{\pi\pi}$ can be done in the following way. Using (6,7) and (11,12) we define components g_A, g_B and h_A, h_B of amplitudes g and h as follows:

$$g \equiv g_A + g_B, \quad g_A \equiv \frac{A}{2M} U \quad g_B \equiv \frac{B}{2} r V, \quad (14)$$

$$h \equiv h_A + h_B, \quad h_A \equiv \frac{A}{2M} U^* \quad h_B \equiv \frac{B}{2} r V^*, \quad (15)$$

where

$$U = (b - a)cs + i(bc^2 + as^2), \quad (16)$$

$$V = (1/a - 1/b)cs - i(s^2/a + c^2/b) \quad (17)$$

with the following shorthand notation: $a = \sqrt{-t_{max}}$, $b = \sqrt{-t_{min}}$, $r = m_f^2 - m_\pi^2$, $c = \cos(\frac{1}{2}\Theta_s)$, $s = \sin(\frac{1}{2}\Theta_s)$.

From (14,15) one can obtain the desired amplitudes $\frac{A}{2M}$ and $\frac{B}{2}r$:

$$\frac{A}{2M} = \frac{1}{W}(gV^* - hV), \quad (18)$$

$$\frac{B}{2}r = \frac{1}{W}(-gU^* + hU), \quad (19)$$

where

$$W = UV^* - U^*V. \quad (20)$$

Solutions (18,19) are well suited for the analysis of experimental data taken with narrow t -bins. The CERN-Cracow-Munich data [26] have been, however, averaged over a relatively wide t -range:

$$t_1 = -0.2 \text{ (GeV/c)}^2 < t < t_2 = -0.005 \text{ (GeV/c)}^2. \quad (21)$$

Therefore, we need amplitudes \bar{g} and \bar{h} averaged over this t -range, where

$$\bar{g} \equiv \frac{1}{t_2 - t_1} \int_{t_1}^{t_2} g(t) dt \quad (22)$$

with similar equation for \bar{h} . Then according to (14-15) we write

$$\bar{g} = \frac{1}{2M} \overline{AU} + \frac{1}{2} r \overline{BV} \quad (23)$$

$$\bar{h} = \frac{1}{2M} \overline{AU^*} + \frac{1}{2} r \overline{BV^*}, \quad (24)$$

where symbols \overline{AU} , \overline{BV} etc. are defined as in (22).

In order to proceed further we have to assume some t -dependence of functions A and B allowing for complete freedom in the effective mass dependence. Thus, we write

$$A(m_{\pi\pi}, t) = A_0(m_{\pi\pi})p(m_{\pi\pi}, t) \quad (25)$$

and

$$B(m_{\pi\pi}, t) = B_0(m_{\pi\pi})q(m_{\pi\pi}, t), \quad (26)$$

where $p(m_{\pi\pi}, t)$ and $q(m_{\pi\pi}, t)$ are postulated functions of t (which may also depend on $m_{\pi\pi}$), $A_0(m_{\pi\pi})$ and $B_0(m_{\pi\pi})$ depend on $m_{\pi\pi}$ only and their behaviour should be determined from experiment. A possible parametrization of $p(m_{\pi\pi}, t)$ is:

$$p(m_{\pi\pi}, t) = \frac{e^{a(m_{\pi\pi})t}}{m_\pi^2 - t}, \quad (27)$$

which is equal to the pion propagator multiplied by the exponential form factor with parameter $a(m_{\pi\pi})$ being an a priori unknown function of $m_{\pi\pi}$. This shape of functional dependence has been introduced in many pion exchange models. For $q(m_{\pi\pi}, t)$ we have used four different parametrizations: 1, t , $\exp(bt)$ and $t \exp(bt)$ with $b=4 \text{ GeV}^{-2}$. As we shall show later, separation of averaged amplitudes \bar{g} and \bar{h} into a sum of averaged parts $\bar{g}_A + \bar{g}_B$ and $\bar{h}_A + \bar{h}_B$ as in (14-15) and (23-24) is largely insensitive to the form of parametrization of function $q(m_{\pi\pi}, t)$. Functions \bar{g}_A , \bar{h}_A , \bar{g}_B and \bar{h}_B are linear combinations of amplitudes \bar{g} and \bar{h} :

$$\bar{g}_A = c_1 \bar{g} + c_2 \bar{h}, \quad (28)$$

$$\bar{h}_A = d_1 \bar{g} + d_2 \bar{h}, \quad (29)$$

$$\bar{g}_B = d_2 \bar{g} - c_2 \bar{h}, \quad (30)$$

$$\bar{h}_B = -d_1 \bar{g} + c_1 \bar{h}, \quad (31)$$

where the complex coefficients are

$$c_1 = \overline{qV^*} \overline{pU}/D, \quad (32)$$

$$c_2 = -\overline{qV} \overline{pU}/D, \quad (33)$$

$$d_1 = \overline{qV^*} \overline{pU^*}/D, \quad (34)$$

$$d_2 = -\overline{qV} \overline{pU^*}/D \quad (35)$$

and

$$D = \overline{pU} \overline{qV^*} - \overline{pU^*} \overline{qV}. \quad (36)$$

Having functions \overline{g} and \overline{h} experimentally determined, Eqs (28-36) make it possible to calculate the unknown functions $A_0(m_{\pi\pi})$ and $B_0(m_{\pi\pi})$ in the following way:

$$\frac{A_0(m_{\pi\pi})}{2M} = \frac{\overline{g_A}}{pU} \quad (37)$$

and

$$\frac{B_0(m_{\pi\pi})}{2} r = \frac{\overline{g_B}}{qV}. \quad (38)$$

From (25-26) we then obtain the desired functions A and B , so that separation of amplitude (3) into pseudoscalar and pseudovector parts is finally achieved.

b) Determination of scalar-isoscalar pion-pion interaction amplitude

Separation of the pseudoscalar amplitude, dominantly corresponding to the one pion exchange contribution to the $\pi^- p \rightarrow f_0 n$ process, is the first step in the determination of the scalar-isoscalar pion-pion amplitude a_0 . This amplitude can be calculated if both the S -wave $\pi^+\pi^- \rightarrow \pi^+\pi^-$ amplitude a_S and the $I=2$ S -wave amplitude a_2 are known:

$$a_0 = 3 a_S - \frac{1}{2} a_2 \quad (39)$$

(see [21] p.12 and notice that the $I=1, S=0$ contribution vanishes). Amplitude a_S is closely related to $A_0/2M$ given by (37) since A_0 is a factor responsible for the $\pi\pi$ interaction in (25):

$$a_S = - \frac{p_\pi \sqrt{s} q_\pi f}{m_{\pi\pi} \sqrt{2} \cdot \frac{g^2}{4\pi}} \frac{A_0}{2M}, \quad (40)$$

where p_π is the incoming π^- momentum in the $\pi^- p$ c.m. frame, q_π is the final pion momentum in the f_0 decay frame, $g^2/4\pi = 14.6$ is the pion-nucleon coupling constant, and f is the correction factor. In this factor the averaged t -dependence of the pion-nucleon vertex function and the off-shellness of the exchanged pion are included, which allows us to apply this formula to the analysis of the data taken in a wide t -region.

When writing (40) we have assumed that absorption effects due to the final state interaction of the $\pi\pi$ with the outgoing neutron can be neglected. This assumption is supported by the results obtained in studies of absorption effects using the Regge phenomenology ([31]). The point is that in the case of

dominance of the nucleon helicity flip amplitude, final state interaction effects are relatively weak. Thus, we can expect that errors caused by those effects are smaller than experimental errors.

Amplitude a_2 can be measured in the process $\pi^+ p \rightarrow \pi^+ \pi^+ n$, provided the partial wave analysis is done and a similar separation of pseudoscalar and pseudovector contributions is performed. Although studies of $\pi^+ \pi^+$ and $\pi^- \pi^-$ systems were in the past [32], the above-mentioned separation, which requires polarization measurements, has never been performed. Therefore, we have to rely on determination of the $I=2$ amplitude based on the assumption that one-pion exchange dominates in the process under discussion. The $I=2$ S -wave amplitude has been calculated using the data of [32] and the pion-pion separable potential model previously applied to the description of the coupled channel $\pi\pi$ and $K\bar{K}$ $I=0$, S -wave interactions [2]. Here for the $I=2$ channel we use a very simple two-parameter pion-pion potential of rank one:

$$V_\pi(p, p') = \lambda G(p)G(p'), \quad (41)$$

where λ is a constant and

$$G(p) = \sqrt{\frac{4\pi}{m_\pi}} \frac{1}{p^2 + \beta^2} \quad (42)$$

is a form factor with one range parameter β ; p and p' are pion c.m. momenta in the initial and final states respectively. The calculated phase shifts δ_2 corresponding to the amplitude

$$a_2 = \sin \delta_2 \exp(i\delta_2) \quad (43)$$

for $\Lambda \equiv \frac{\lambda}{2\beta^3} = -0.1309$ and $\beta = 3.384$ GeV are shown in Fig. 1. The analytical form of the amplitude a_2 can be found in Appendix A of [2]. This amplitude, along with a_S obtained from (40), was used to calculate a_0 given by (39). Amplitude a_2 , being generally smaller than a_S , cannot be, however, neglected in (39) as shown in Sect. 4 d. Amplitude a_0 is normalized to Argand's form:

$$a_0 = \frac{\eta e^{2i\delta} - 1}{2i}, \quad (44)$$

where δ is the $I=0$, $S=0$ phase shift and η is the inelasticity coefficient.

3 Model-independent determination of partial-wave amplitudes

This section is a short recapitulation of what was extensively described in the old papers of the CERN-Cracow-Munich collaboration [26, 30, 33, 34], to which the reader is referred for more details.

In the analysis, 3×10^5 events on a hydrogen target[20] were combined with 1.2×10^6 events on a polarized (butanol) target, both for 17.2 GeV/c π^- . The former events yield t_M^L moments while the latter provide the p_M^L and r_M^L moments from interactions with protons of hydrogen bound in butanol molecule (protons in carbon and oxygen nuclei cannot be polarized). In this way we obtain a quasi-complete description of the reaction:

$$\pi^- p_{\uparrow} \rightarrow \pi^+ \pi^- n. \quad (45)$$

In the case of a transversely polarized target the differential cross section can be written as

$$\frac{d^2\sigma}{dm_{\pi\pi} dt d\Omega} = \sum_{L,M} t_M^L \text{Re} Y_M^L(\Omega) + P \cos\psi \sum_{L,M} p_M^L \text{Re} Y_M^L(\Omega) + P \sin\psi \sum_{L,M} r_M^L \text{Im} Y_M^L(\Omega), \quad (46)$$

where:

$m_{\pi\pi}$ - effective mass of the $\pi^+\pi^-$ system,

t - four-momentum transfer squared from the π^- beam to the $\pi^+\pi^-$ system,

Y_M^L - spherical harmonics,

Ω - decay angles of the π^- in the t-channel $\pi^+\pi^-$ rest frame,

ψ - polarization angle,

P - degree of polarization.

Table 1

Number of parameters and observables in partial-wave analysis, l denotes the π^- orbital momentum in the $\pi^+\pi^-$ rest frame and m - its projection.

$l_{max}(\text{wave})$	1(P)	2(D)	3(F)
Number of amplitudes ($m \leq 1$)	8	14	20
Number of real parameters ($m \leq 1$)	14	26	38
Number of t_M^L moments ($M \leq 2$)	6	12	18
Number of p_M^L moments ($M \leq 2$)	6	12	18
Number of r_M^L moments ($M \leq 2$)	3	7	11
Total number of moments ($M \leq 2$)	15	31	47

Moments of angular distribution t_M^L , p_M^L and r_M^L are bilinear combinations of partial wave amplitudes. As described in the previous Section, we use nucleon transversity amplitudes g and h corresponding to a given naturality exchange. It should be stressed that the number of t_M^L moments is smaller (see Table 1) than the number of real parameters characterizing the amplitudes,

and therefore model-independent partial-wave analysis is not possible. Consequently, all $\pi^+\pi^-$ phase shift studies that do not use polarized target data were based on non-trivial physical assumptions like vanishing of spin-nonflip amplitudes (in our language this corresponds to $g_i \equiv h_i$, where i denotes l, m) in the unnatural spin-parity amplitudes and phase coherence between the $m = 0$ and $m = 1$ amplitudes. It was shown in [18, 26, 30] that these assumptions are badly broken by the polarized-target data. Unfortunately, this fact has been ignored in all subsequent $\pi\pi$ studies with the notable exception of Svec papers [17, 18].

On the other hand, additional knowledge of p_M^L and r_M^L moments yields the total number of observables which, as seen in Table 1, slightly exceeds the number of real parameters. Since the present analysis is restricted to low t , we can ignore all $m > 1$ amplitudes as all $M > 2$ moments vanish (for a high- t study see [35]).

Terms appearing in amplitude combinations are of the type $|g_i|^2$, $|h_i|^2$, $Re(g_i g_j^*)$ or $Re(h_i h_j^*)$ but there is no mixed term like $Re(g_i h_j^*)$. Consequently, we cannot determine the relative phase between the g and h amplitudes in a model-independent way but the transversity amplitudes can be completely determined *independently within each set*. This includes moduli and *relative phases* with the warning that all the relative phases within each set can be multiplied by -1 .

In the analysis we expect to find some discreet ambiguities that arise from bilinearity of the equations. In order not to lose any solution, great effort was devoted to providing many different starting points to the MINUIT program [36]. They were as follows (see [33] for details):

- i) exact analytical solutions (possible for $l_{max} = 1$ only),
- ii) approximate analytical solution assuming that intensity of the P_0 wave is much smaller than that of the S and D_0 -waves (for $l_{max} = 2$),
- iii) approximate analytical solution assuming phase coherence (for $l_{max} = 2$ and $l_{max} = 3$),
- iv) several sets of random values,
- v) results of the fit from neighbouring bins.

It should be stressed that approximations in ii) and iii) were used for finding the starting values *only; it was always the exact formulae that were fitted*. In [26] such fits were done in 40 MeV bins for

$$580 \text{ MeV} < m_{\pi\pi} < 1780 \text{ MeV}$$

$$0.01 \text{ GeV}^2/c^2 < |t| < 0.20 \text{ GeV}^2/c^2.$$

Later, similar analysis was performed in finer mass bins ($\Delta m_{\pi\pi} = 20 \text{ MeV}$) in a slightly different kinematical region, i.e.

$$600 \text{ MeV} < m_{\pi\pi} < 1600 \text{ MeV}$$

$$0.005 \text{ GeV}^2/c^2 < |t| < 0.200 \text{ GeV}^2/c^2.$$

The fits became more difficult and time-consuming as higher partial waves were included; therefore, the MINOS error analysis (see [36] for details) was required for all parameters for $l_{max} = 1$ only. For higher masses, when more waves were needed, the MINOS errors were calculated for the leading $m = 0$ waves only. The solution was considered to be acceptable only if the MINOS error analysis was possible; the χ^2 values, being generally good, were hardly helpful in selecting solutions. Quite often there was only one such solution in a given bin, although many different starting points were used. However, in the mass region below $f_0(980)$ there are two branches of solutions, best seen in the moduli of the S-wave g and h amplitudes around 900 MeV. This reflects the old "up-down" ambiguity.

Intensities $I_i = |g_i|^2 + |h_i|^2$ of partial waves obtained in the 20 MeV analysis were published in [34], in fact they still represent the most accurate measurements of the $f_2(1270)$ parameters [29]. Moduli and relative phases of transversity amplitudes are used in this paper for the first time.

4 Results

a) Determination of the S -wave

In Figs 2–4 we show the experimental results obtained by the CERN–Cracow–Munich collaboration as described in the previous Section. Independent variables used in their partial wave analysis were: the sum $|\bar{g}|^2 + |\bar{h}|^2$ (Fig. 2a), the ratio $|\bar{g}|/|\bar{h}|$ (Fig. 2b), as well as the phase differences $\vartheta_g^L - \vartheta_g^{L'}$ and $\vartheta_h^L - \vartheta_h^{L'}$ ($L, L' = S, P, D, F$) (Figs 3 and 4). In our analysis we have assumed that phases of the partial waves are described mainly by phases of the final state interaction amplitude of the $\pi\pi$ system. It means in particular that phases of the P , D and F -waves follow phases of $\rho(770)$, $f_2(1270)$ and $\rho_3(1690)$ decay amplitudes into $\pi\pi$. Our PWA has been done in three $m_{\pi\pi}$ effective mass regions from 600 MeV to 1600 MeV.

i) 600 MeV – 980 MeV

In this region one can safely assume that only the S and P -waves contribute since the D -wave is weak even at the upper limit of this region. It is only in this region that fully analytical solutions of the PWA equations are possible

[33]. The PWA analysis however, yields two solutions ("up" and "down") which are distinctly different in the $m_{\pi\pi}$ region from 800 MeV to 980 MeV. In the "up" solution the sum $|\bar{g}|^2 + |\bar{h}|^2$ exhibits a maximum for $m_{\pi\pi} \approx 770$ MeV, but in the "down" solution the moduli of $|\bar{g}|^2$ and $|\bar{h}|^2$ are roughly constant from about 750 MeV to 980 MeV. The shape of the S -wave "up" modulus was used by Svec to claim the existence of the $f_0(750)$ meson [16, 17].

S -wave phases of reaction (2) have been determined from phase differences between S and P -waves. In addition to the "up-down" ambiguity in the moduli of the \bar{g} and \bar{h} transversity amplitudes, there is also a phase ambiguity in each $m_{\pi\pi}$ bin. This ambiguity comes from the mathematical structure of the PWA equations from which only cosines of the relative phases of the partial waves of reaction (2) can be obtained. In our analysis we present two arbitrary choices of the S -wave phases which form data sets shown in Figs 3 and 4. In the first set, called "steep", S -wave phases grow faster than P -wave phases. In the other set, called "flat", increase in S -wave phases is slower than that for P -waves. Thus two sets of possible phases ("flat" or "down") combined with two branches of moduli ("up" and "down") lead us to consideration of four solutions for the amplitudes g and h which can be called "up-steep", "down-steep", "up-flat" and "down-flat". Following this splitting of the amplitudes also the $\pi - \pi$ phase shifts which will be derived from them will be similarly labelled. In order to avoid a possible future confusion let us remark here that in many papers in past the words "up" and "down" served mainly to distinguish the S -wave phase-shifts: the values of the phase shifts "up" were larger than the corresponding values of the solution "down". However, in the models in which the a_1 exchange has been neglected and the S -wave amplitude was assumed elastic, the modulus of the "up" amplitude $\pi^- p \rightarrow \pi^- \pi^+ n$ was *smaller* than the modulus of the amplitude "down" for the effective $\pi^- \pi^+$ mass larger than about 800 MeV. The reason of this correlation can be understood if we remember that the phase shifts of the "down" solution were close to 90° while the phase shifts of the "up" solution were considerably larger in that effective mass range and the modulus of the amplitude was proportional to $|\sin \delta|$. In our case, however, we do not neglect an important contribution of the a_1 exchange, so we have more combinations of the possible solutions for the amplitudes g and h .

ii) 980 MeV - 1460 MeV

Here, the S , P and D -waves have been included in the PWA analysis. In this region the $f_2(1270)$ production is very strong so the D -wave dominates and the S -wave phases have been evaluated from phase differences between the S and D -waves. In our model we have assumed that in the 980 MeV - 1460 MeV region differences between the P and D -wave are positive since the

phase of the $\rho(770)$ meson decay amplitude into two pions is larger than the corresponding phase of the $f_2(1270)$ meson amplitude. This allowed us to fix the sign of phase difference between the S and D -waves in each energy bin, thus avoiding phase ambiguity present in the first region.

iii) 1460 MeV – 1600 MeV

Here, the S , P , D and F (dominated by the $\rho_3(1690)$ meson) waves have been included in the PWA analysis. Consequently, the S -wave phases have been calculated from phase differences between the S and F -waves. The sign of each difference has been fixed by the assumption that phase differences between the P and F -waves as well as between the D and F -waves are positive.

In each of the three regions production amplitudes of the $\rho(770)$, $f_2(1270)$ and $\rho_3(1690)$ resonances follow the Breit-Wigner parametrisation of [26, 34], namely

$$M = \sqrt{A} \frac{m_{\pi\pi}}{\sqrt{q}} \frac{\sqrt{2l+1} m_R x_R \Gamma}{m_R^2 - m_{\pi\pi}^2 - i m_R \Gamma}, \quad l = 1, 2, 3, \quad (47)$$

where

$$\Gamma = \Gamma_R \left(\frac{q}{q_R} \right)^{2l+1} \frac{D_l(q_R r)}{D_l(qr)}, \quad (48)$$

and the Blatt-Weisskopf functions $D_l(qr)$ have the form:

$$\begin{aligned} D_1(qr) &= 1 + (qr)^2 && \text{for } P\text{-wave,} \\ D_2(qr) &= 9 + 3(qr)^2 + (qr)^4 && \text{for } D\text{-wave,} \\ D_3(qr) &= 225 + 45(qr)^2 + 6(qr)^4 + (qr)^6 && \text{for } F\text{-wave.} \end{aligned} \quad (49)$$

In (47) A is a normalization constant, m_R , Γ_R and x_R are mass, width and inelasticity of the resonance R ($R=\rho(770)$, $f_2(1270)$ or $\rho_3(1690)$), q is momentum of any pion in the $\pi\pi$ rest system, and q_R stands for momentum q for $m_{\pi\pi} = m_R$. Range parameter r for $\rho(770)$ is equal to 4.8 GeV^{-1} for the "up" solution, and 5.3 GeV^{-1} for the "down" solution [34]. For the $f_2(1270)$ and $\rho_3(1690)$ resonances r equals 10 GeV^{-1} and 3 GeV^{-1} respectively [26].

Simultaneous presence of the P and D -waves for $m_{\pi\pi} > 980 \text{ MeV}$ allowed us to check the validity of parametrisation of the P and D -wave phases by resonant amplitudes (47). In Fig. 5 we have shown phase differences between the P and D waves for \bar{g} and \bar{h} transversity amplitudes. The P and D -waves in the \bar{h} transversity amplitude are well described by the $\rho(770)$ and $f_2(1270)$ resonant amplitudes but in the case of the \bar{g} amplitude such parametrisation is not sufficient.

Since in the PWA analysis there is no phase relation between the \bar{g} and \bar{h} transversity amplitudes, we have defined the S -wave phases in the following

way:

$$\vartheta_g^S = \begin{cases} \vartheta_g^S - \vartheta_g^P + \theta_{\rho(770)} & \text{for } 600 \text{ MeV} \leq m_{\pi\pi} \leq 980 \text{ MeV}, \\ \vartheta_g^S - \vartheta_g^D + \theta_{f_2(1270)} + \Delta & \text{for } 980 \text{ MeV} \leq m_{\pi\pi} \leq 1460 \text{ MeV}, \\ \vartheta_g^S - \vartheta_g^F + \theta_{\rho_3(1690)} & \text{for } 1460 \text{ MeV} \leq m_{\pi\pi} \leq 1600 \text{ MeV}, \end{cases} \quad (50)$$

$$\vartheta_h^S = \begin{cases} \vartheta_h^S - \vartheta_h^P + \theta_{\rho(770)} + \Delta & \text{for } 600 \text{ MeV} \leq m_{\pi\pi} \leq 980 \text{ MeV}, \\ \vartheta_h^S - \vartheta_h^D + \theta_{f_2(1270)} + \Delta & \text{for } 980 \text{ MeV} \leq m_{\pi\pi} \leq 1460 \text{ MeV}, \\ \vartheta_h^S - \vartheta_h^F + \theta_{\rho_3(1690)} & \text{for } 1460 \text{ MeV} \leq m_{\pi\pi} \leq 1600 \text{ MeV} \end{cases} \quad (51)$$

In (50) and (51) $\theta_{\rho(770)}$, $\theta_{f_2(1270)}$ and $\theta_{\rho_3(1690)}$ are phases of the resonant amplitudes defined in (47). Function Δ has the form:

$$\Delta = \begin{cases} 50.37^\circ & \text{for } 600 \text{ MeV} \leq m_{\pi\pi} \leq 990 \text{ MeV}, \\ 50.37^\circ - 0.116^\circ(m_{\pi\pi} - 990 \text{ MeV}) & \text{for } 990 \text{ MeV} \leq m_{\pi\pi} \leq 1420 \text{ MeV}, \\ 0 & \text{for } m_{\pi\pi} \geq 1420 \text{ MeV}. \end{cases} \quad (52)$$

Function Δ has been introduced in order to parametrize the differences between $(\vartheta_h^P - \vartheta_h^D)$ and $(\vartheta_g^P - \vartheta_g^D)$. We have determined this function empirically from a linear fit in the range of $980 \text{ MeV} \leq m_{\pi\pi} \leq 1300 \text{ MeV}$.

b) Separation of the S -wave into pseudoscalar- and pseudovector-exchange components

Transversity amplitudes \bar{g} and \bar{h} have been averaged over t as it was described in Sect. 2. Coefficients c_1, c_2, d_1 and d_2 depend on averages \overline{pU} and \overline{qV} , and therefore they also depend on the form of functions $p(t)$ and $q(t)$. We have checked the dependence of amplitudes $\overline{g_\alpha}, \overline{h_\alpha}$ ($\alpha = A, B$) and A, B on the value of parameter a (Eq. 27) for $0 \leq a \leq 4 \text{ GeV}^{-2}$. For both "up" and "down" solutions and for both "flat" and "steep" sets of the S -wave phases below 1000 MeV, the differences in moduli and phases of amplitudes $\overline{g_A}, \overline{h_A}$ and $\overline{g_B}, \overline{h_B}$ are not higher than 3% for $600 \text{ MeV} \leq m_{\pi\pi} \leq 1600 \text{ MeV}$. In the case of the A amplitude the differences between different solutions can reach 10%. We have evaluated parameter a to be 3.5 GeV^{-2} from experimental data [30] in the mass range of $710 \text{ MeV} < m_{\pi\pi} < 830 \text{ MeV}$. Since we do not know its mass dependence outside this region, we have kept it fixed to 3.5 GeV^{-2} in the whole $m_{\pi\pi}$ range.

We have also checked the dependence of pseudoscalar and pseudovector exchange amplitudes on the form of function $q(t)$ for the following functions: $q(t) = 1, t, e^{bt}$ and $q(t) = te^{bt}$, where $b = 4 \text{ GeV}^{-2}$. The second and fourth forms come from parametrization of the Regge propagator for the a_1 exchange

at $t \approx 0$ [31]. Differences in moduli and phases of the A , \overline{g}_A , \overline{h}_A , \overline{g}_B and \overline{h}_B amplitudes caused by different functional forms of $q(t)$ are smaller than 5%. Very small changes of amplitude B (smaller than 0.5%) are due to the strong factorization of the average $\overline{qV} \simeq \overline{q}\overline{V}$. Therefore, in the numerical calculations we have chosen $q(t) = 1$.

Parameter f introduced in (40) has an influence on amplitudes a_0 and a_S defined in Sect. 2. We have evaluated this parameter by minimizing differences $1 - \eta$ for $600 \text{ MeV} \leq m_{\pi\pi} \leq 990 \text{ MeV}$ for each solution ("up" and "down") combined with the phase set ("flat" and "steep") separately.

Since the dependence of transversity amplitudes \overline{g}_α and \overline{h}_α ($\alpha = A, B$) on the shape of functions $p(t)$ and $q(t)$ is weak, we have used them to separate contributions of one-pion and a_1 exchanges. Amplitudes \overline{g}_α and \overline{h}_α depend on moduli and relative phases of amplitudes \overline{g} and \overline{h} . Since for $m_{\pi\pi} < 980 \text{ MeV}$ there are two solutions for moduli ("up" and "down") and two solutions for relative phases ("flat" and "steep"), we obtain four combinations of amplitudes which will be further labelled "up-flat", "up-steep", "down-flat" and "down-steep". In Fig. 6 and 7 the moduli and phases of these four amplitudes are shown.

c) Properties of pseudoscalar- and pseudovector-exchange amplitudes

Separation of amplitudes leads to the equality of corresponding moduli: $|\overline{h}_A| = |\overline{g}_A|$ and $|\overline{h}_B| = |\overline{g}_B|$ (see Eqs 14 and 15). However, phases of \overline{h}_A and \overline{h}_B differ from the corresponding phases of \overline{g}_A and \overline{g}_B . Their differences, being functions of the effective mass, are related to the phases of complex coefficients c_i and d_i ($i = 1, 2$ in Eqs 28–35). The first phase difference, defined as the phase of \overline{h}_A minus the phase of \overline{g}_A , increases monotonically from about 10° to 50° in the effective mass range from 600 MeV to 1600 MeV. The second phase difference, defined as the phase of \overline{h}_B minus the phase of \overline{g}_B , is almost constant ($\approx -174^\circ$) in the whole region of the effective mass. This behaviour follows from the fact that the imaginary part of coefficient U (Eq. 16) is much smaller than the real part of U , and the imaginary part of coefficient V dominates over its real part (Eq. 17). Since we assume that functions $p(t)$ and $q(t)$ are real, the phase of amplitude A is the arithmetic average of the \overline{g}_A and \overline{h}_A phases while that of amplitude B is the arithmetic average of the \overline{g}_B and \overline{h}_B phases (compare Eqs 14 and 15). Their values differ strongly between four sets of solutions. The \overline{g}_A phases systematically increase for the $\pi\pi$ effective mass between 600 MeV and about 980 MeV. Sudden phase change and strong reduction of the \overline{g}_A moduli for $m_{\pi\pi} \simeq 1000 \text{ MeV}$ results from the appearance of the narrow resonance $f_0(980)$. Similarly decrease in the phases and moduli of amplitudes \overline{g}_A for $m_{\pi\pi} > 1400 \text{ MeV}$ can be related

to the presence of another scalar resonance of mass between 1400 MeV and 1500 MeV. In most cases, errors of the phases and moduli of \bar{g}_A are smaller than the corresponding errors for \bar{g}_B .

The a_1 exchange amplitude \bar{g}_B amounts on average to about 20% of the pion exchange amplitude but around 1000 MeV and 1500 MeV it is of the same order as \bar{g}_A . A slight increase in the \bar{g}_B modulus and a decrease in the \bar{g}_A modulus for the effective mass above 1420 MeV (seen in Figs 6 a,b and 7 a,b) can be related to the presence of a scalar resonance $f_0(1500)$ coupled to channels such as $\pi\pi$, $\eta\eta$, $\eta\eta'$ and 4π (or $\sigma\sigma$) [5], [10] – [12]. On the basis of the $p\bar{p} \rightarrow 5\pi^0$ annihilation data, S. Resag from the Crystal Barrel Collaboration [11] suggested a possible coupling of the $f_0(1500)$ to $\pi(1300)\pi$, where $\pi(1300)$ couples in turn to $(\pi\pi)_S\pi$ with $(\pi\pi)_S$ denoting the $\pi\pi$ pair in the $I = 0, S$ -state. The possible enhancement of the $|\bar{g}_B|$ amplitude seen in Figs 6 and 7 above 1400 MeV can be, however, attributed to another decay mode of $f_0(1500)$, namely to a system $a_1\pi$, where $a_1 \rightarrow (\pi\pi)_S\pi$. However, the small value of the partial decay width of a_1 into $(\pi\pi)_S\pi$, which – according to the Particle Data Group [29] – is equal to 0.3% of the total a_1 width, is questionable. This number follows from just one analysis [37] related to the not well confirmed four-quark model of Jaffe [38]. The data gathered by the ACCMOR collaboration [39] for reaction $\pi^-p \rightarrow 3\pi p$ indicate a much larger a_1 coupling to $(\pi\pi)_S\pi$ (even several tens in percent of the total a_1 width). In reaction $\pi^-p \rightarrow \pi^+\pi^-n$ a possible subprocess is the a_1 exchange followed by interaction $\pi^-a_1 \rightarrow (\pi^+\pi^-)_S$ in the isoscalar state. It seems therefore the pseudovector exchange process can also contribute to possible production of the $f_0(1500)$ scalar resonance in the reaction under consideration.

d) Pseudoscalar $I = 0, S$ -wave amplitudes

Finally, let us extract the $\pi\pi$ scalar-isoscalar amplitude a_0 from pseudoscalar amplitude \bar{g}_A just separated from pseudovector amplitude \bar{g}_B . We use formulae (37) and (39)–(44) to obtain phase shifts δ and inelasticity coefficient η corresponding to a_0 . In Fig. 8 we show the dependence of those parameters on the effective mass for solutions labelled "steep" (corresponding to a fairly steep behaviour of the phases of amplitudes \bar{g} and \bar{h}). For both solutions ("up-steep" and "down-steep") we observe a characteristic fast increase of phase shifts near 760 MeV (see Figs 8 a,b). Now all the solutions have to pass a test connected with the fitting of the complex coefficient $f = |f| e^{i\varphi}$ to the requirement that the inelasticity coefficient $\eta = 1$ in the whole mass range from $m_{\pi\pi} = 600$ MeV to the $K\bar{K}$ production threshold.

It appears immediately that the "down-steep" solution fails this test. Such an attempt leads to unacceptably high $\chi^2/NDF = 80/17$ value obtained in the best case for $|f| = 0.78$ and $\varphi = -8.4^\circ$. In addition, there

is a strange behavior of η i.e. a clear violation of unitarity constraint below $m_{\pi\pi} < 720$ MeV and above 820 MeV while $\eta < 1$ between these two values (see Fig. 8 c). It should be noted that if we changed normalization to keep $\eta \leq 1$ in the whole mass range in question we would deal with a puzzling large inelasticity between $m_{\pi\pi} = 720$ MeV and 820 MeV. Therefore, in our opinion the "down-steep" solution is nonphysical and should be excluded.

The situation is different for the "up-steep" solution, for which we can find a constant factor such that η does not deviate from unity ($\chi^2/NDF = 15/17$) for $|f| = 0.73$ and $\varphi = -9.2^\circ$. However, also here we observe a puzzling behaviour with η systematically exceeding unity for $m_{\pi\pi} < 720$ MeV and above $m_{\pi\pi} = 820$ MeV but staying below 1 in the intermediate mass range.

On the other hand both "flat" solutions exhibit natural behavior with η fluctuating around unity. In addition, minimizing the $\eta - 1$ differences below the $K\bar{K}$ production threshold we obtain reasonable values of f close to 1, namely $|f| = 0.89$, $\varphi = -4.4^\circ$ for the solution "up" and $|f| = 0.84$, $\varphi = -17.8^\circ$ for the solution "down". Thus we are left with two favoured, nicely behaving, solutions ("up-flat" and "down-flat") and one, somewhat queer, but still acceptable "up-steep" solution. Let us remark that *only* the last solution is consistent with the relatively narrow $f_0(750)$ meson¹ claimed by Svec [17, 18] on the basis of *moduli* of transversity amplitudes determined with the help of the polarized-target data.

In all solutions there is a sudden drop in η for the effective mass near 1000 MeV, caused by an opening of a new $K\bar{K}$ channel. Another decrease of η can be seen above 1500 MeV.

In Figs. 8 a,b and 9 a,b the phase shifts δ for all solutions have been compared with those obtained from the analysis of the $\pi^-p \rightarrow \pi^+\pi^-n$ reaction on an *unpolarized* target [20] (solution B), where separation of the π -exchange and a_1 -exchange amplitudes was impossible. In Fig. 9 b in the mass region from 600 MeV to about 1400 MeV we see only minor differences between phase shifts corresponding to the "down-flat" solution and the results of [20]. In the "up-flat" solution around 900 MeV, however, the values of δ are higher than those of ref.[20] by several tens of degrees as seen in Fig. 9 a (a qualitatively similar difference led many years ago to the "up-down" nomenclature). The "up-steep" solution (see Fig. 8 a) with a narrow resonance is entirely different from the results of ref.[20]. Let us notice that the characteristic "jump" of the "up-steep" phase shifts at 980 MeV is smaller (about 100°) than those in the the "up-flat" ($\approx 120^\circ$) and "down-flat" ($\approx 140^\circ$) solutions.

Finally let us comment on the behaviour of the phase shifts at higher effective masses, well above the $K\bar{K}$ threshold. Here the different solutions

¹Following the PDG convention we call this object $f_0(750)$ instead of $\sigma(750)$ used in the original papers.

are quite close each other. This follows from our assumption about the phase difference between the D- and S-waves (formulated in Sect. 4a ii) and rather small differences between the phases φ of the factor f (eq. 40).

A short comment on the comparison of errors obtained for the phase shifts in this study and errors obtained in [20] is in order here. Errors in the partial wave analysis [34] have been obtained from the MINOS subroutine of the MINUIT program used to fit data independently in each effective mass bin. Although the errors of the B analysis in [20] are smaller, they do not include systematic effects corresponding to simplifying assumptions like, for example, dominance of the s-channel nucleon helicity flip amplitude and phase coherence of unnatural spin-parity exchange amplitudes with helicity 0 and 1. In our analysis we avoid these assumptions which have been found to be badly broken by the polarized target data already in [26],[30],[34].

Finally, let us note that the $I = 2$, S-wave amplitude a_2 plays an important role in the determination of amplitude a_0 (Eq. 39). In particular, especially at high effective masses, it influences the inelasticity parameter η very much. As described above, phases of amplitude a_2 have been obtained in the experiment on an unpolarized target [32]. Thus, they contain some unknown errors related to the unknown contribution of the a_1 exchange. We feel, however, that those errors can be less important than other errors of amplitude a_S calculated from \bar{g}_A (Eqs 40 and 37).

e) Resonance interpretation of results

Let us now discuss behaviour of phase shifts and inelasticity coefficients in terms of the scalar $I=0$ resonances, both already known and those newly postulated (see Figs 8 and 9).

Systematic increase in phase shifts below 1000 MeV can be related to the existence of a broad σ meson which we have found in [2] and called $f_0(500)$. In [2] we analysed data obtained on an unpolarized target. Applying now the same model to the "down-flat" and "up-flat" solutions obtained for the polarized target we obtain parameters of the $f_0(500)$ meson very similar to those given in [2]. In this way, presence of $f_0(500)$ is reinforced. We should mention here that N. A. Törnqvist and M. Roos [19] also support the existence of the σ meson naming it tentatively $f_0(400 - 900)$. The σ meson of mass 555 MeV has also been reported recently by Ishida et al. ([40]) in an analysis of the $\pi\pi$ phase shifts especially near the pion-pion threshold. The threshold behaviour of the scalar $I=0$ scattering amplitudes is very much influenced by the presence of the $f_0(500)$ state (see [41]). The σ meson plays also a very important role in nuclear physics and in the description of nucleon-nucleon interactions. For example, in [42] typical value of 550 MeV has been used for its mass, which is in agreement with the above findings.

Since our "up-steep" solution (see Sec. 5d) corresponds to the narrow $f_0(750)$ claimed by Svec on the basis of (mainly) the same data let us comment on the similarities and differences of two approaches. Svec uses an "analytical solution+Monte Carlo" method to extract amplitudes from experimental moments while our amplitudes come from the standard χ^2 minimization method. The advantage of the latter is an applicability to higher mass range where more partial waves contribute and analytical solution is not possible. In the very recent draft[18] he compares both methods for $m_{\pi\pi} < 900$ MeV finding an excellent agreement between two methods. But there is an important difference in the further analysis. Svec finds narrow $f_0(750)$ in *only one of two* transversity amplitudes and argues against summing the squares of two amplitude moduli, which - according to him - distorts or even hides the $f_0(750)$. In our analysis we extract the dominating π -exchange amplitude and weaker but non-negligible a_1 -exchange amplitude from connecting *both* transversity amplitudes. Studying the *pure* π -exchange amplitude we find one, less favoured but still possible, solution exhibiting the narrow $f_0(750)$. A simple Breit-Wigner fit with the energy-independent background yields $m = (770 \pm 8)$ MeV and $\Gamma = (120 \pm 9)$ MeV, well consistent with $m = (753 \pm 19)$ MeV and $\Gamma = (108 \pm 53)$ MeV in Ref. [18]. This solution, however, cannot be well described by the above-mentioned model of Ref. [2] without a substantial modification of the pion-pion interaction.

As can be seen in Fig. 9 c, a sudden drop in inelasticity for the effective mass near 1000 MeV is caused by the opening of a new $K\bar{K}$ channel. This fact, along with a characteristic jump of phase shift δ coupled with a rapid decrease in elasticity η near 1000 MeV (Fig. 9 a,b), is due to the narrow $f_0(980)$ resonance [2, 29]. We stress that this jump, although smaller than in two "flat" solutions, is seen *also in the "up-steep" solution*, since in some older studies the "up" solution was rejected as inconsistent with the narrow $f_0(980)$. Analysing the polarized target data Svec has shown that an intensity of one S-wave transversity amplitude can be simultaneously parametrized in terms of two interfering resonances $f_0(750)$ and $f_0(980)$ [18].

Another decrease in η near 1500 MeV – 1600 MeV can be related to the opening of further channels like 4π ($\sigma\sigma$ or $\rho\rho$), $\eta\eta'$ or $\omega\omega$. For $m_{\pi\pi}$ larger than 1470 MeV, phase shifts for both solutions ("up-flat" and "down-flat") show a systematically steeper increase than phase shifts corresponding to data obtained on the unpolarized target. Both facts may be related to the possible existence of the $f_0(1500)$ resonance [4, 5], [10]–[12].

5 Summary

A formalism permitting extraction and separation of the S -wave pseudoscalar and pseudovector exchange amplitudes in the reaction $\pi^- p_{\uparrow} \rightarrow \pi^+ \pi^- n$ on a transversely polarized target has been presented. A new analysis of the CERN–Cracow–Munich collaboration data obtained with 20 MeV bins at 17.2 GeV/c π^- beam momentum on the polarized target has been performed in the $\pi\pi$ energy range from 600 MeV to 1600 MeV. Already at the level of moduli this analysis yields two solutions between 600 MeV and 980 MeV (the “up-down” ambiguity).

Due to the lack of information on the relative phases between transversity amplitudes \bar{g} and \bar{h} we have assumed that the relative phases of both S -wave transversity amplitudes g and h are generally governed by the phase behaviour of the dominant resonant P , D and F partial wave amplitudes corresponding to the $\rho(770)$, $f_2(1270)$ and $\rho_3(1690)$ resonances decaying to the $\pi\pi$ pairs and interfering with the S -wave. This leads to an additional twofold ambiguity since the relative phases can be either added or subtracted. Thus we have “down-flat”, “down-steep”, “up-flat” and “up-steep” solutions. However the “down-steep” solution is shown to violate unitarity and can be ignored. The remaining three solutions are acceptable although the the “up-steep” one exhibits a peculiar behavior of inelasticity.

The a_1 exchange amplitudes are especially important at 1000 MeV and 1500 MeV and cannot be neglected with respect to the π exchange amplitudes. This puts in serious doubt all the PWA results which assumed absence of the a_1 exchange.

Separation of the π -exchange from the a_1 -exchange allowed us to calculate the $I = 0$, S -wave $\pi\pi$ amplitudes in a weakly-model-dependent manner. In the low-mass region both “flat” solutions are consistent with $f_0(500)$ while the phase behavior of the “up-steep” one agrees with the narrow $f_0(750)$. Up to the energy of about 1420 MeV, phase shifts of our “down-flat” solution agree within the errors with the one obtained without the polarized-target data. However, above 1420 MeV the phase shifts in all solutions increase with energy faster than those obtained without the polarized-target data. This phase behavior as well as an increase of the a_1 -exchange amplitude can be due to the presence of the $f_0(1500)$.

Acknowledgements. We thank L. Görlich, J. Kwieciński, B. Loiseau, M. Rózańska and J. Turnau for enlightening discussions and communications. We are also grateful to Dr. Svec for sending us his papers prior to publication and for calling our attention to the narrow $f_0(750)$ meson.

This work has been partially supported by the Polish State Committee for

Scientific Research (grants No 2 P03B 231 08, 2 P03B 043 09) and by the Maria Skłodowska–Curie Fund II (No PAA/NSF–94–158).

References

- [1] J. Weinstein and N. Isgur: Phys. Rev. **D27** (1983) 588
- [2] R. Kamiński, L. Leśniak and J.-P. Maillet: Phys. Rev. **D50** (1994) 3145
- [3] V. V. Anisovich *et al.* (Crystal Barrel Coll.): Phys. Lett. **B323** (1994) 233
- [4] C. Amsler: in *Proceedings of XXVII International Conference on High Energy Physics*, Glasgow 1994, eds P. Bussey and I. G. Knowles, Bristol: Institute of Physics Publishing, Ltd 1995 p. 199
- [5] C. Amsler and F. E. Close: Phys. Rev. **D53** (1996) 295
- [6] G. Bali *et al.*: Phys. Lett. **B309** (1994) 29
- [7] J. Sexton, A. Vaccarino and D. Weingarten: "Numerical evidence for the observation of a scalar glueball", IBM preprint IBM-HET-95-2; see also D. Weingarten, Nucl. Phys. **B34** (*Proc. Suppl.*) (1994) 29
- [8] N. A. Törnqvist: "Summary of Gluonium '95 and Hadron '95 conferences", talk given at the *International Europhysics Conference on High Energy Physics*, Brussels, July 27 –August 2, 1995, hep-ph/9510256
- [9] M. R. Pennington: report No DPT-95/86, to appear in *Proceedings of 6th International Conference on High Energy Physics (HADRONS '95)*, Manchester, England, 10–14 July 1995, hep-ph/9510229
- [10] D. V. Bugg *et al.*: to appear in *Proceedings of 6th International Conference on High Energy Physics (HADRONS '95)*, Manchester, England, 10–14 July 1995
- [11] S. Resag: to appear in *Proceedings of 6th International Conference on High Energy Physics (HADRONS '95)*, Manchester, England, 10–14 July 1995
- [12] C. Amsler *et al.*, (Crystal Barrel Coll.): Phys. Lett. **B291** (1992) 347, Phys. Lett. **B322** (1994) 431, Phys. Lett. **B342** (1995) 433, Phys. Lett. **B353** (1995) 571, Phys. Lett. **B355** (1995) 425
- [13] F. Antinori *et al.*, (WA91 Coll.): Phys. Lett. **B353** (1995) 589

- [14] N. A. Törnqvist: Zeit. Phys. **C68** (1995) 647
- [15] V. V. Anisovich *et al.*: Phys. Lett. **B364** (1995) 195
- [16] M. Svec, A. de Lesquen and L. van Rossum: Phys. Rev. **D46** (1992) 949
- [17] M. Svec, Phys. Rev. **D53**, 2343 (1996).
- [18] M. Svec, "Mass and Width of $\sigma(750)$ Scalar Meson from Measurements of $\pi N \rightarrow \pi^- \pi^+ N$ on Polarized Targets", hep-ph/9607297.
- [19] N. A. Törnqvist and M. Roos: Phys. Rev. Lett. **76** (1996) 1575
- [20] G. Grayer *et al.*: Nucl. Phys. **B75** (1974) 189
- [21] B.R. Martin, D. Morgan and G. Shaw: in *Pion-pion interactions in particle physics*. London: Academic Press 1976
- [22] V. Srinivasan *et al.*: Phys. Rev. **D12** (1975) 681
- [23] B. Hyams *et al.*: Nucl. Phys. **B100** (1975) 205
- [24] P. Estabrooks and A. D. Martin: Nucl. Phys. **B79** (1974) 301
- [25] W. Ochs: Nuovo Cim. **12A** (1972) 724
- [26] H. Becker *et al.*: Nucl. Phys. **B151** (1979) 46
- [27] M. R. Pennington and S. D. Protopopescu: Phys. Rev. **D7** (1973) 2591
- [28] D. Morgan: Nuovo Cim. **107A** (1994) 1883
- [29] Particle Data Group: Phys. Rev. **D54** (1996) 1
- [30] H. Becker *et al.*: Nucl. Phys. **B150** (1979) 301
- [31] A. C. Irving and R. P. Worden: Phys. Rep. **34 C** (1977) 118
- [32] W. Hoogland *et al.*: Nucl. Phys. **B69** (1974) 266, Nucl. Phys. **B126** (1977) 109
- [33] G. Lutz and K. Rybicki: "Nucleon polarization in the reaction $\pi^- p_{\uparrow} \rightarrow \pi^+ \pi^- n$ ", MPI report MPI-PAE/Exp.El.75, October 1978
- [34] V. Chabaud *et al.*: Nucl. Phys. **B223** (1983) 1
- [35] K. Rybicki and I. Sakrejda: Z. Phys. **C28** (1985) 65

- [36] F. James and M. Roos: Computer Physics Communications **10** (1975) 343
- [37] R. S. Longacre: Phys. Rev. **D26** (1982) 82
- [38] R. L. Jaffe: Phys. Rev. **D15** (1977) 267
- [39] C. Daum *et al.*, (ACCMOR Collaboration): Nucl. Phys. **B182** (1981) 269
- [40] S. Ishida *et al.*: "An Analysis of $\pi\pi$ -scattering Phase Shift and Existence of σ (555) Particle", KEK Preprint 95-183, NUP-A-95-13, Dec. 1995
- [41] R. Kamiński and L. Leśniak: Phys. Rev. **C51** (1995) 2264 and H. Niewodniczański Institute of Nuclear Physics report No 1675/PH, "Low energy parameters of the $K\bar{K}$ and $\pi\pi$ scalar-isoscalar interactions", June 1994
- [42] R. Machleidt, K. Holinde and Ch. Elster: Phys. Rep. **149** (1987) 1

FIGURE CAPTIONS

- Fig. 1. The $I = 2$, S -wave $\pi\pi$ phase shifts versus the effective $\pi\pi$ mass. The curve represents the fit to the data [32].
- Fig. 2. Results of the partial wave analysis of the CERN–Cracow–Munich collaboration: **a)** $|\bar{g}|^2 + |\bar{h}|^2$, **b)** ratio $|\bar{g}| / |\bar{h}|$. Below 980 MeV, full and open circles represent the "down" and "up" solution, respectively.
- Fig. 3. Phase differences of the g transversity amplitudes obtained in the partial wave analysis of the CERN–Cracow–Munich collaboration: **a)** Solution "up": phase differences $\vartheta_g^S - \vartheta_g^P$ between the S and P -waves for the "flat" set (full circles) and the "steep" set (open circles), phase differences $\vartheta_g^S - \vartheta_g^D$ between the S and D -waves (diamonds) and phase differences $\vartheta_g^S - \vartheta_g^F$ between the S and F -waves (squares). **b)** Solution "down": notation as in a).
- Fig. 4. Phase differences of the h transversity amplitudes obtained in the partial wave analysis of the CERN–Cracow–Munich collaboration. Notation as in Fig. 3. **a)** Solution "up". **b)** Solution "down".
- Fig. 5. Phase differences between the P and D -waves for the g ($\vartheta_g^P - \vartheta_g^D$: open circles) and h ($\vartheta_h^P - \vartheta_h^D$: full circles) transversity amplitudes versus the effective $\pi\pi$ mass. Dashed line represents the effective $\pi\pi$ mass dependence of function Δ obtained from a fit to differences $(\vartheta_h^P - \vartheta_h^D) - (\vartheta_g^P - \vartheta_g^D)$ denoted by triangles. Solid line represents differences between phases of the $\rho(770)$ and $f_2(1270)$ decay amplitudes.
- Fig. 6. **a)** Moduli of pseudoscalar $|\bar{g}_A| = |\bar{h}_A|$ (open circles) and pseudovector $|\bar{g}_B| = |\bar{h}_B|$ (diamonds) exchange amplitudes as a function of the effective $\pi\pi$ mass for the "up–flat" solution. **b)** Same as in a) for the "up–steep" solution. **c)** Phases of pseudoscalar exchange amplitudes \bar{g}_A (open circles) and pseudovector amplitudes \bar{g}_B (diamonds) versus the effective $\pi\pi$ mass for the "up–flat" solution. **d)** Same as in c) for the "up–steep" solution. **e)** The phases of the pseudoscalar exchange amplitudes \bar{h}_A (open circles) and the pseudovector amplitudes \bar{h}_B (diamonds) versus the effective $\pi\pi$ mass for the "up–flat" solution. **f)** Same as in e) for the "up–steep" solution.
- Fig. 7. **a)** Moduli of pseudoscalar $|\bar{g}_A| = |\bar{h}_A|$ (full circles) and pseudovector $|\bar{g}_B| = |\bar{h}_B|$ (diamonds) exchange amplitudes as a function of the effective $\pi\pi$ mass for the "down–flat" solution. **b)** Same as in

a) for the "down-steep" solution. **c)** Phases of pseudoscalar exchange amplitudes $\overline{g_A}$ (full circles) and pseudovector amplitudes $\overline{g_B}$ (diamonds) versus the effective $\pi\pi$ mass for the "down-flat" solution. **d)** Same as in c) for the "down-steep" solution. **e)** Phases of pseudoscalar exchange amplitudes $\overline{h_A}$ (full circles) and pseudovector amplitudes $\overline{h_B}$ (diamonds) versus the effective $\pi\pi$ mass for the "down-flat" solution. **f)** Same as in e) for the "down-steep" solution.

- Fig. 8. **a)** Scalar-isoscalar $\pi\pi$ phase shifts δ_0^0 as a function of the effective $\pi\pi$ mass for the "up-steep" solution (open circles) and for data [20] (triangles). **b)** Same as in a) for the "down-steep" solution (full circles). **c)** Scalar-isoscalar $\pi\pi$ inelasticity coefficient η versus the effective $\pi\pi$ mass for the "down-steep" (full circles) and "up-steep" (open circles) solutions.
- Fig. 9. **a)** Scalar-isoscalar $\pi\pi$ phase shifts δ_0^0 as a function of the effective $\pi\pi$ mass for the "up-flat" solution (open circles) and for data [20] (triangles). **b)** Same as in a) for the "down-flat" solution (full circles). **c)** Scalar-isoscalar $\pi\pi$ inelasticity coefficient η versus the effective $\pi\pi$ mass for the "down-flat" (full circles) and "up-flat" (open circles) solutions.

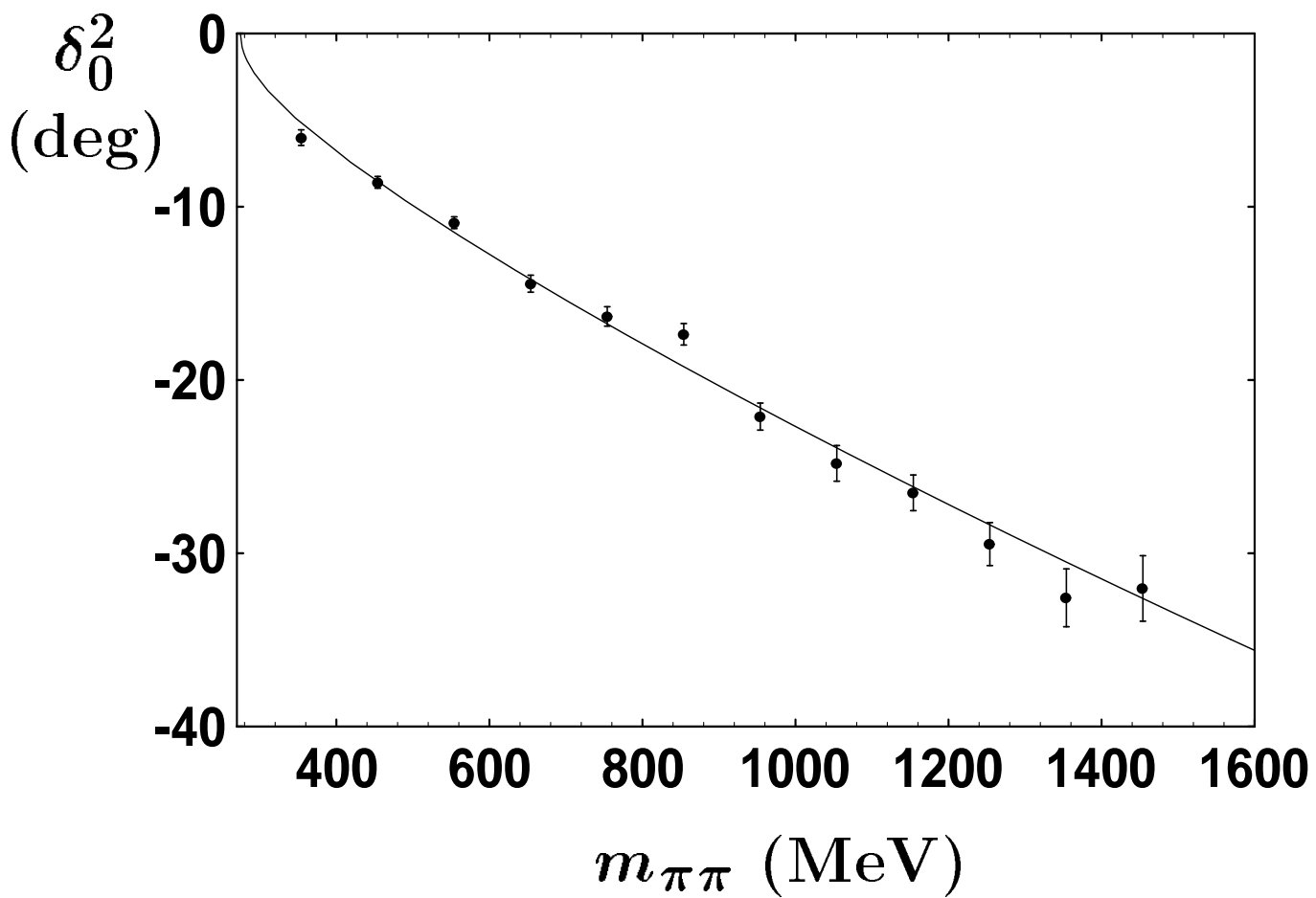


Fig. 1

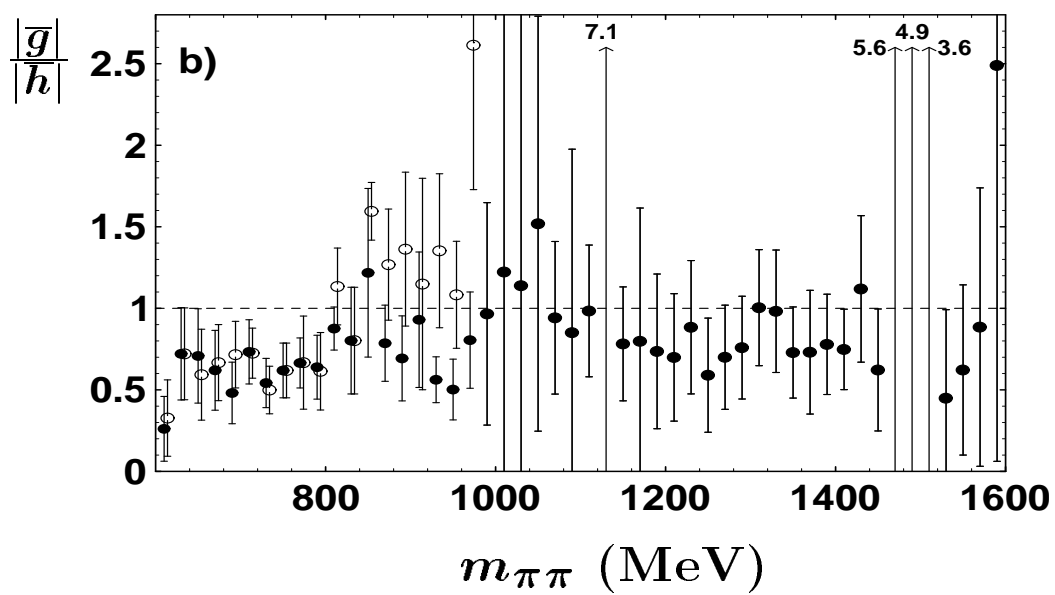
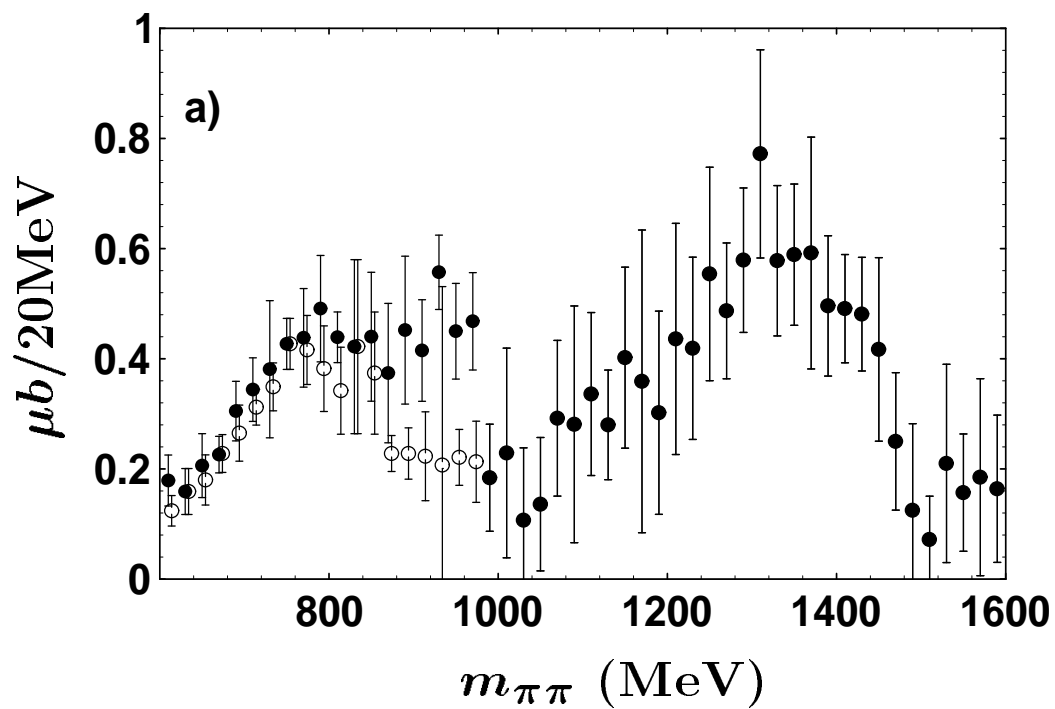


Fig. 2

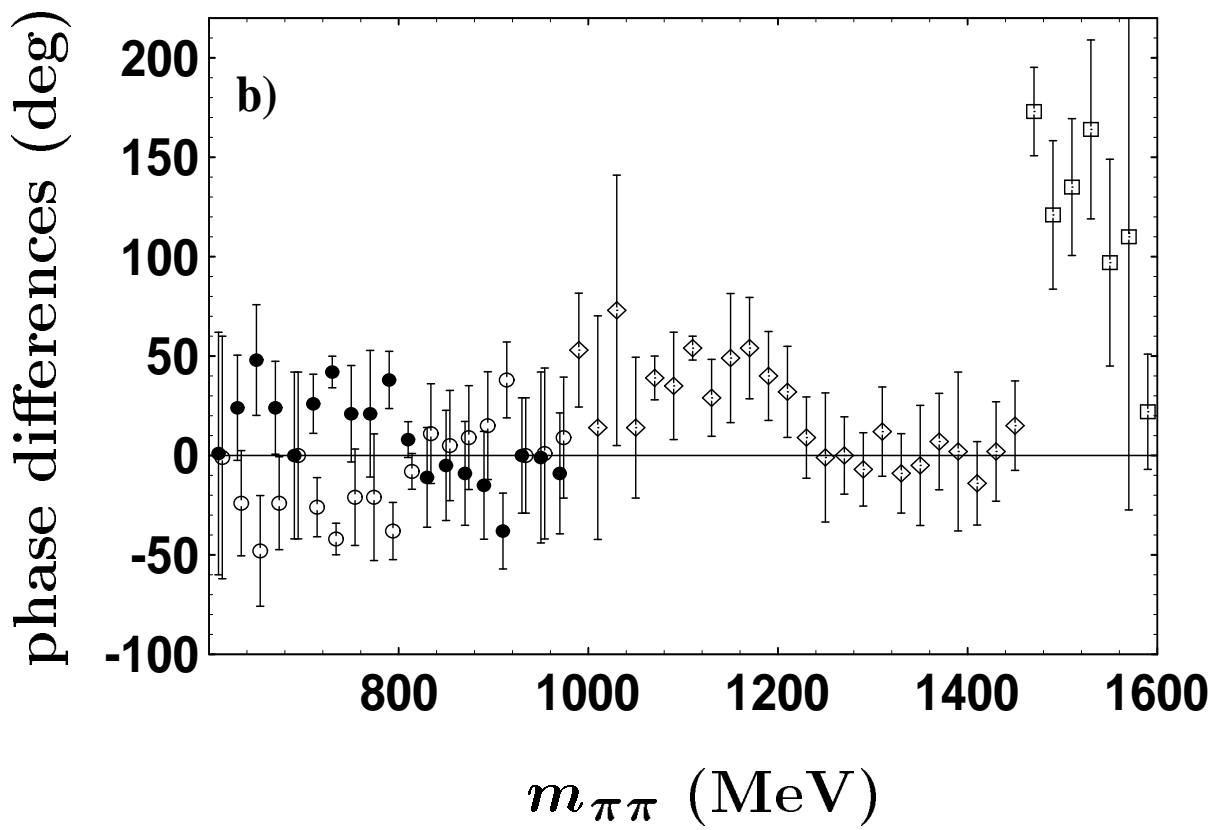
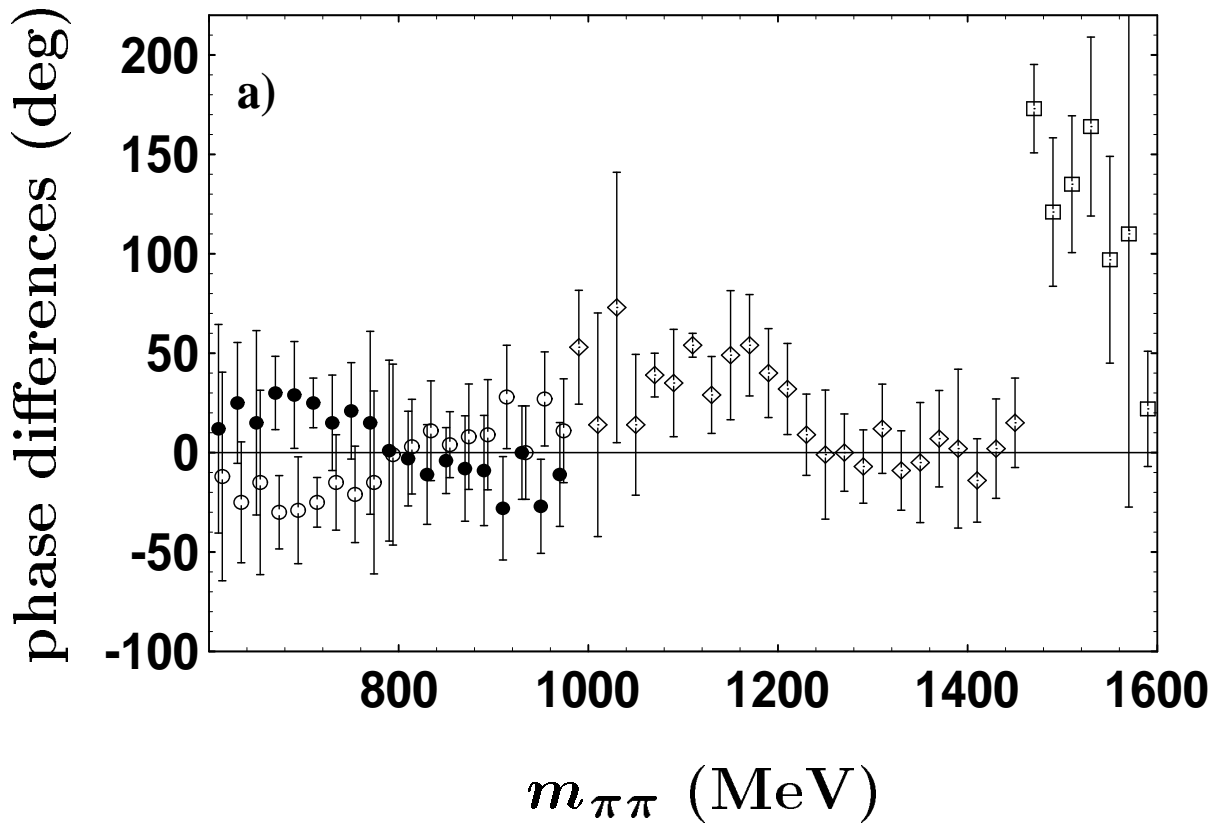


Fig. 3

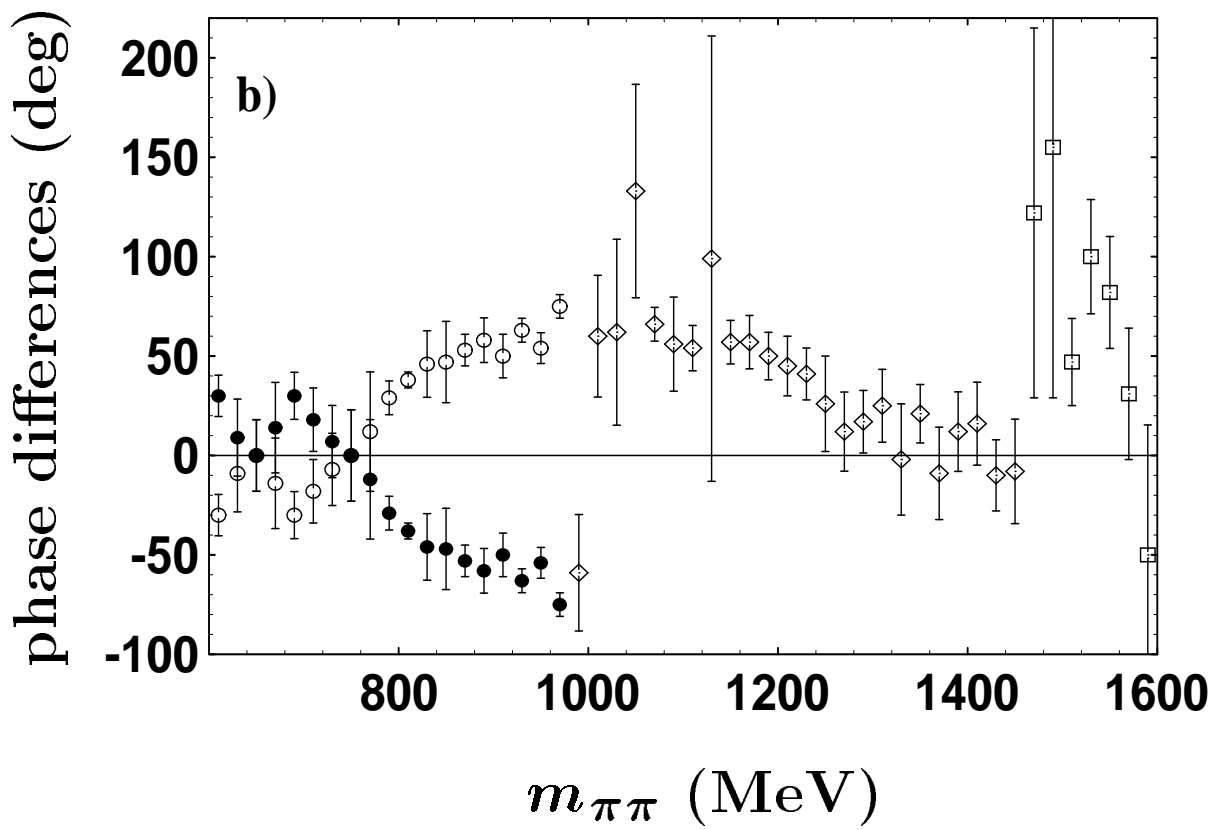
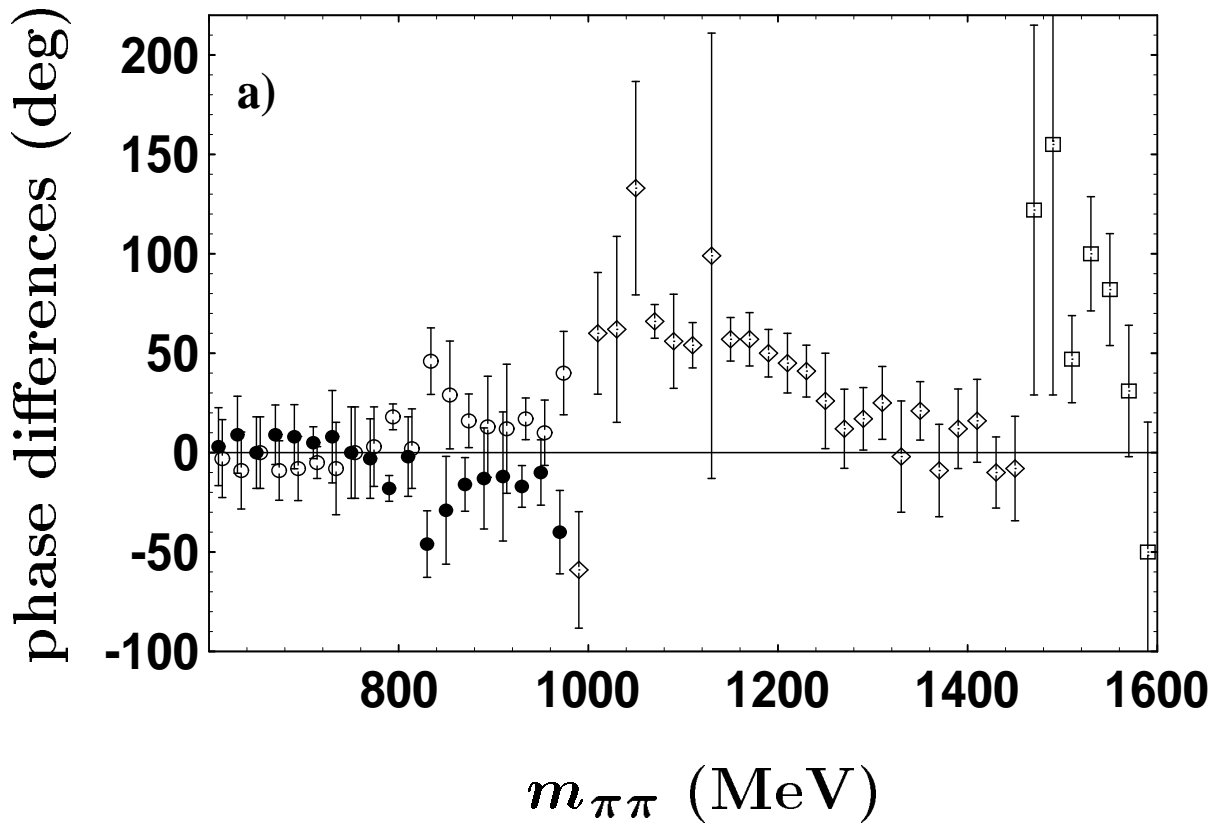


Fig. 4

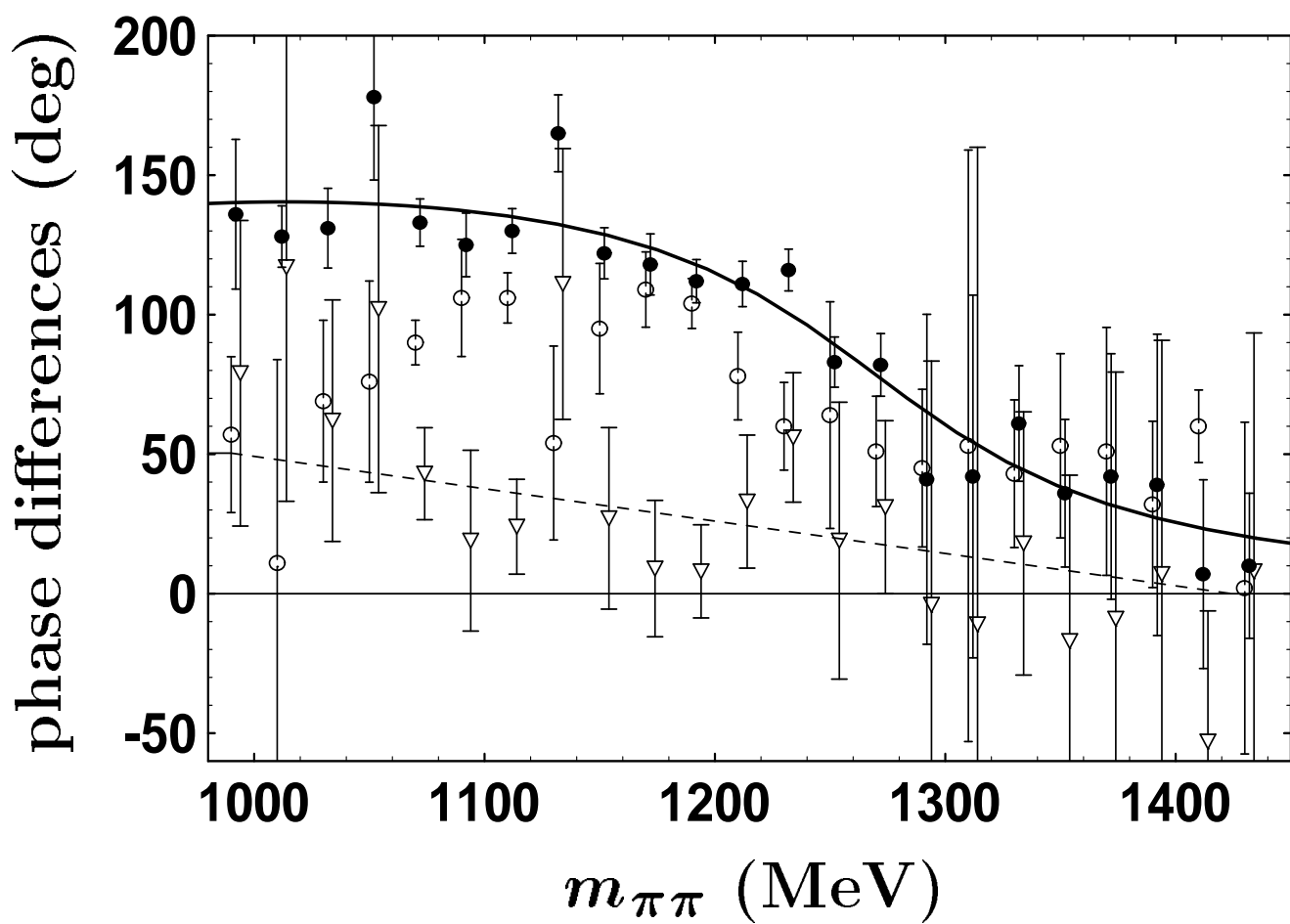


Fig. 5

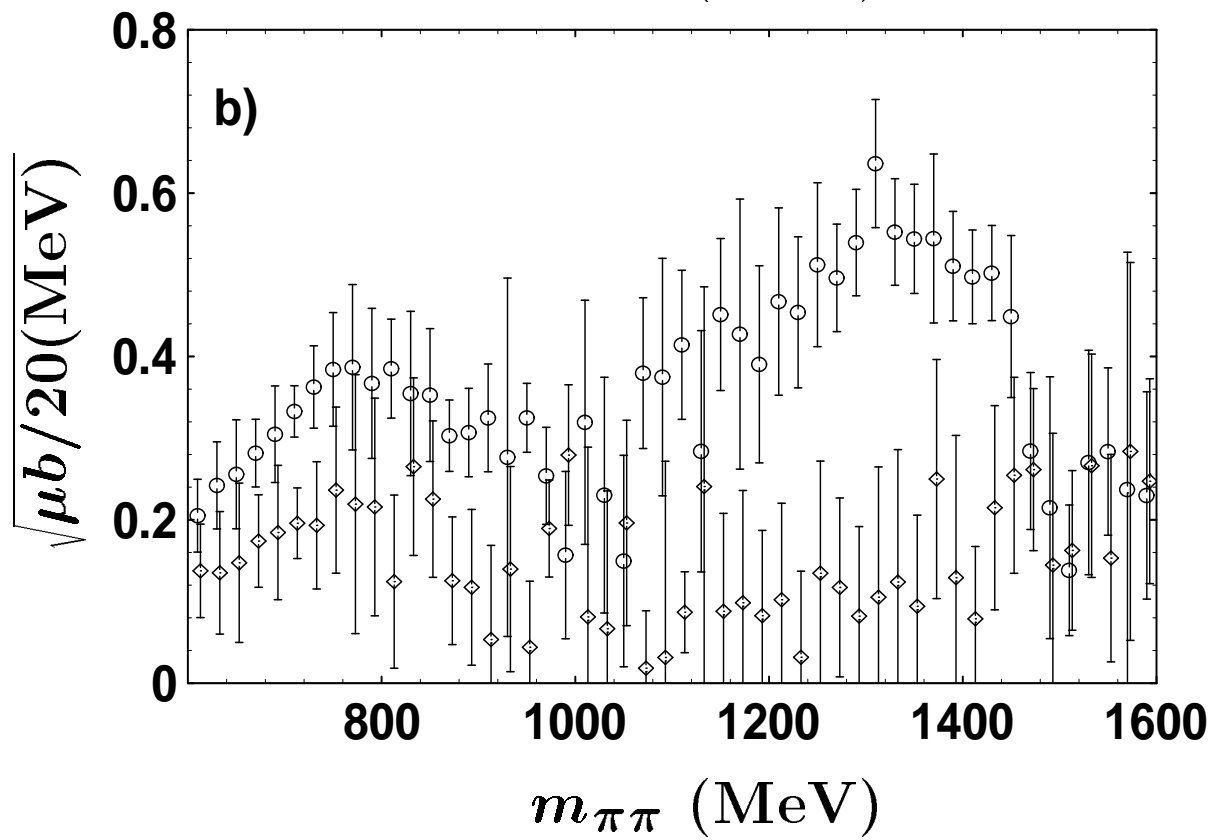
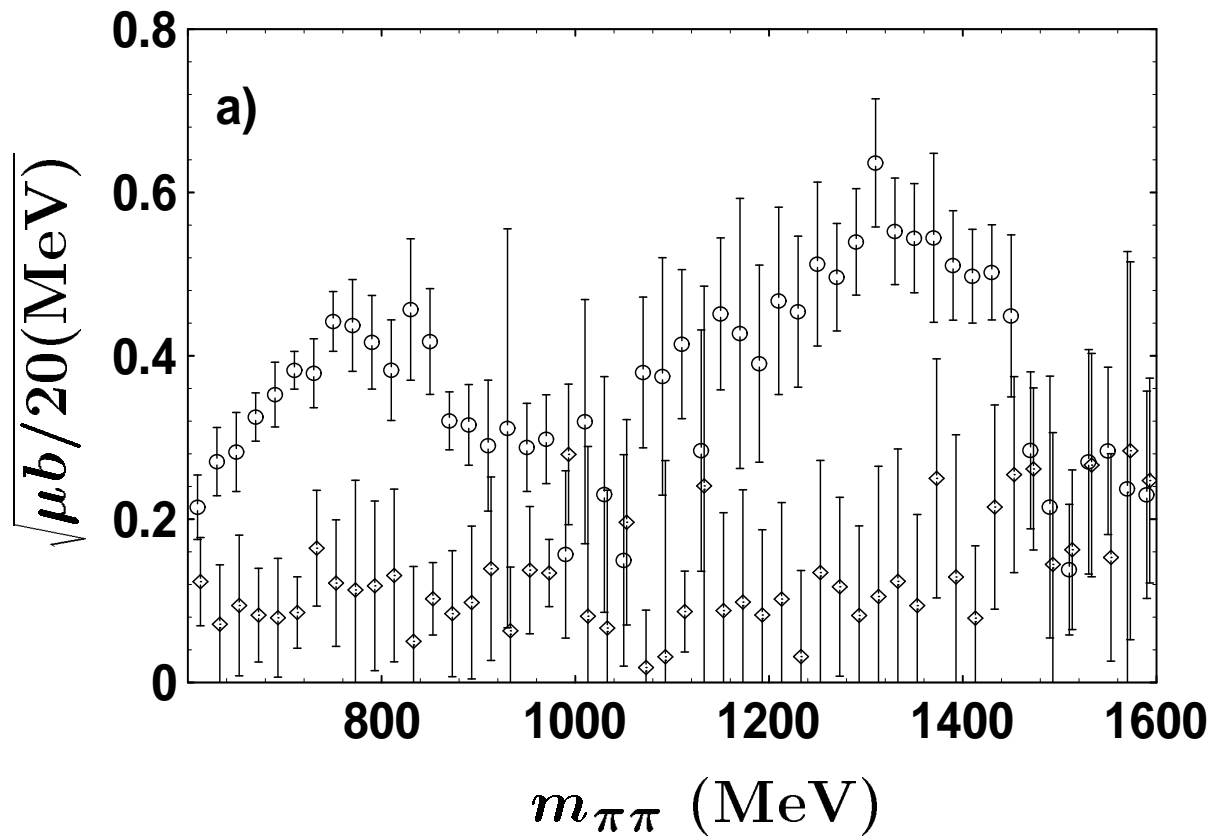


Fig. 6ab

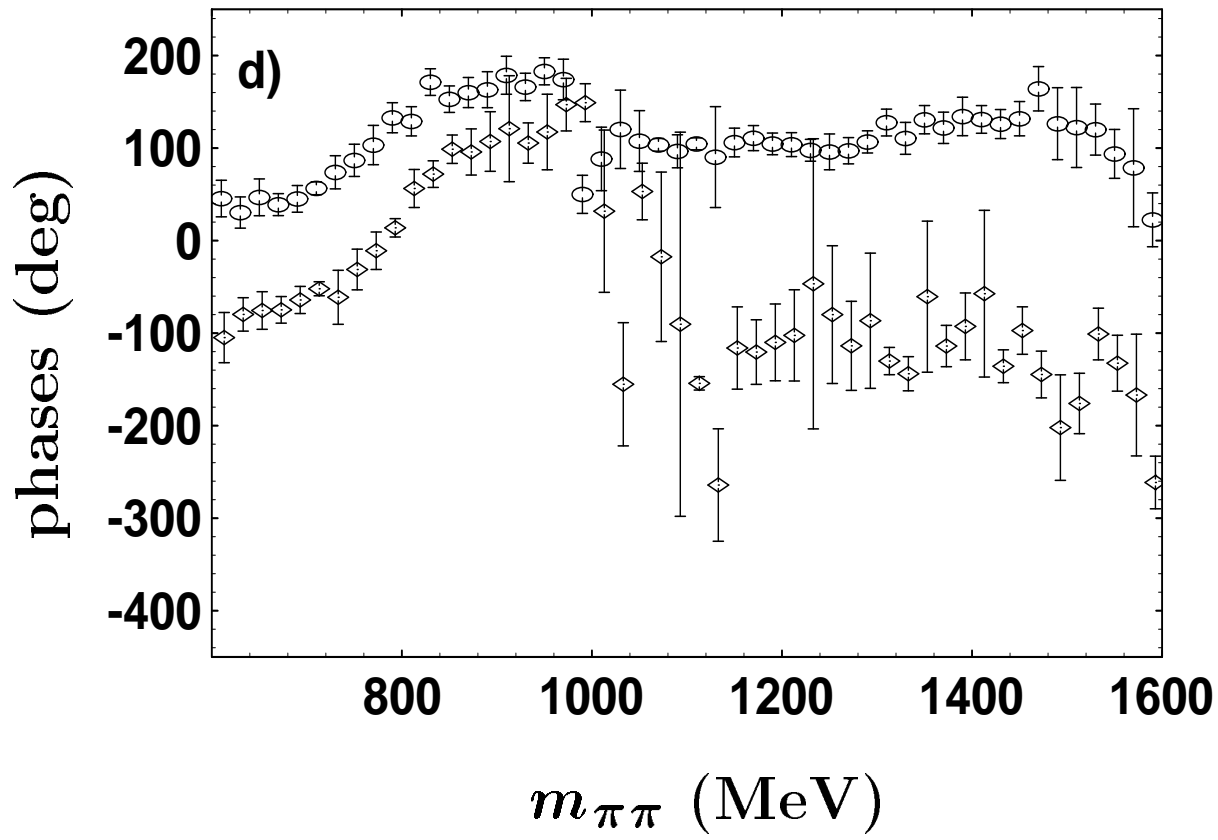
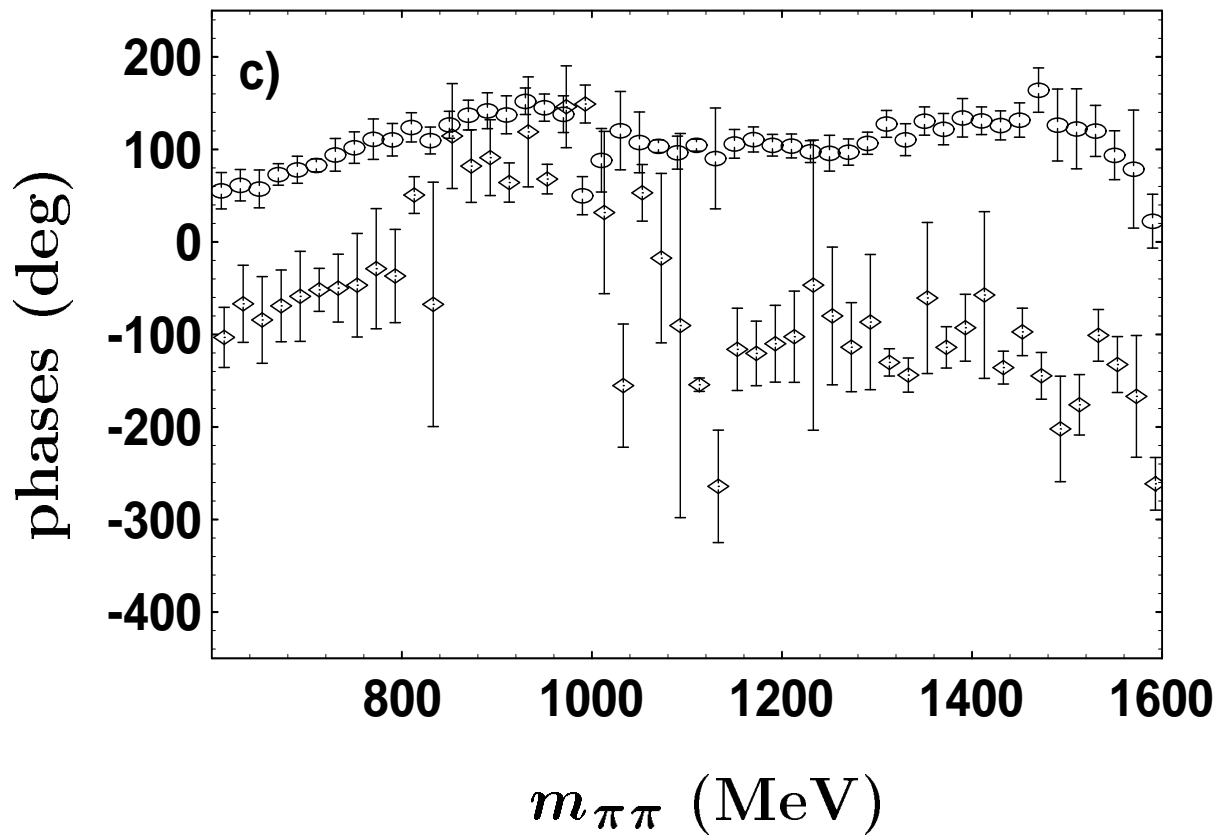


Fig. 6cd

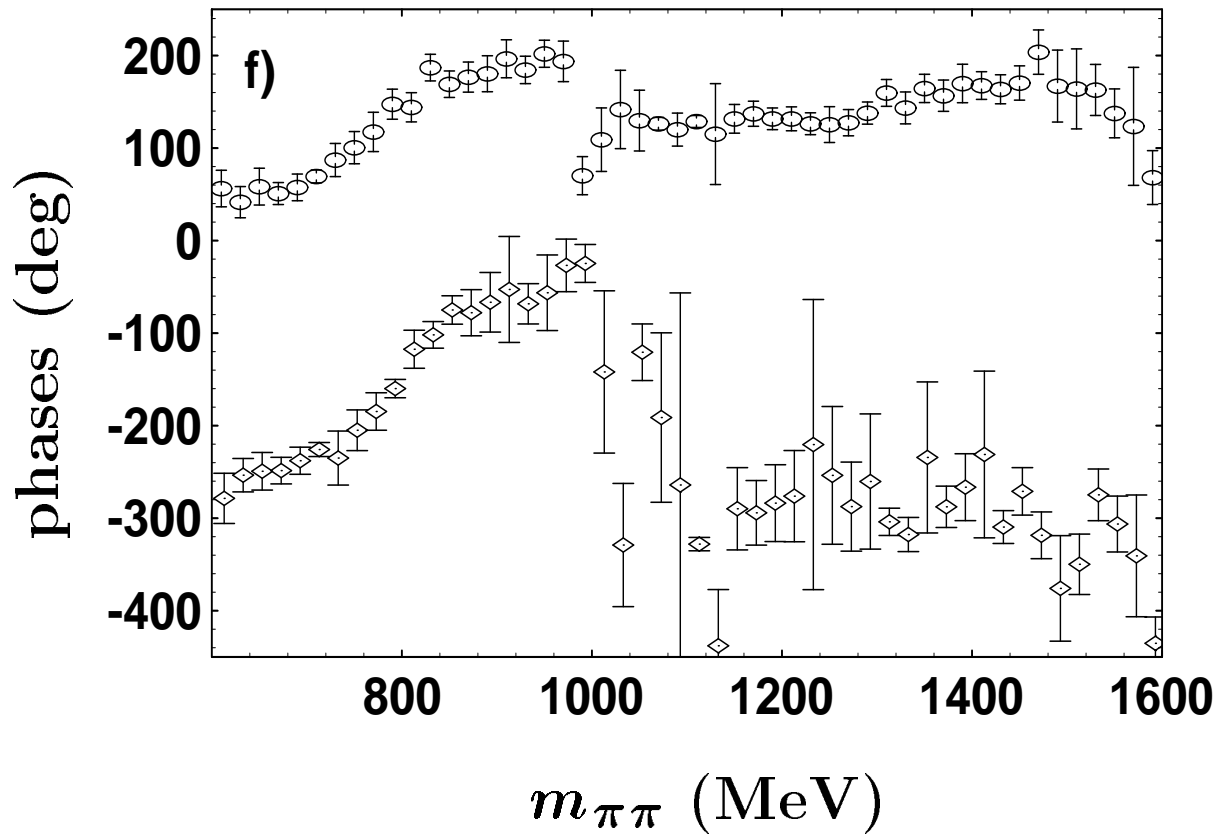
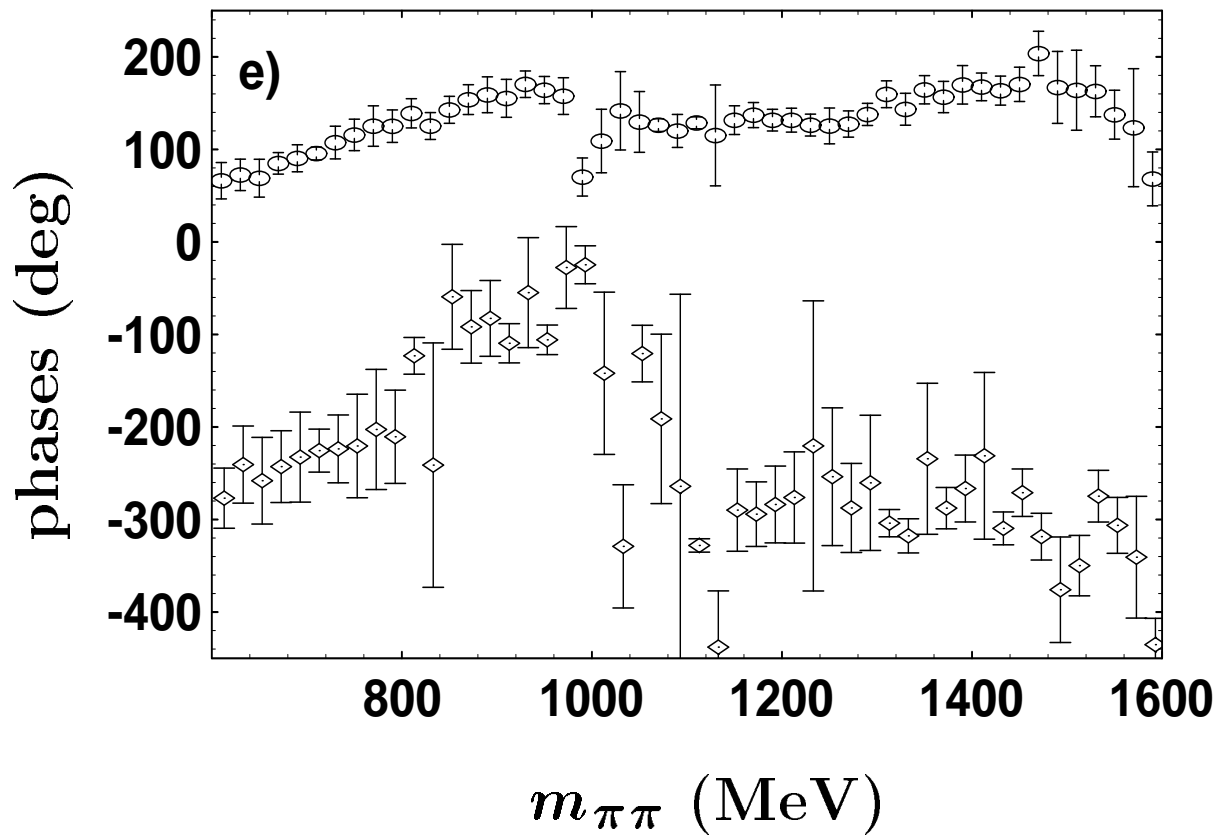


Fig. 6ef

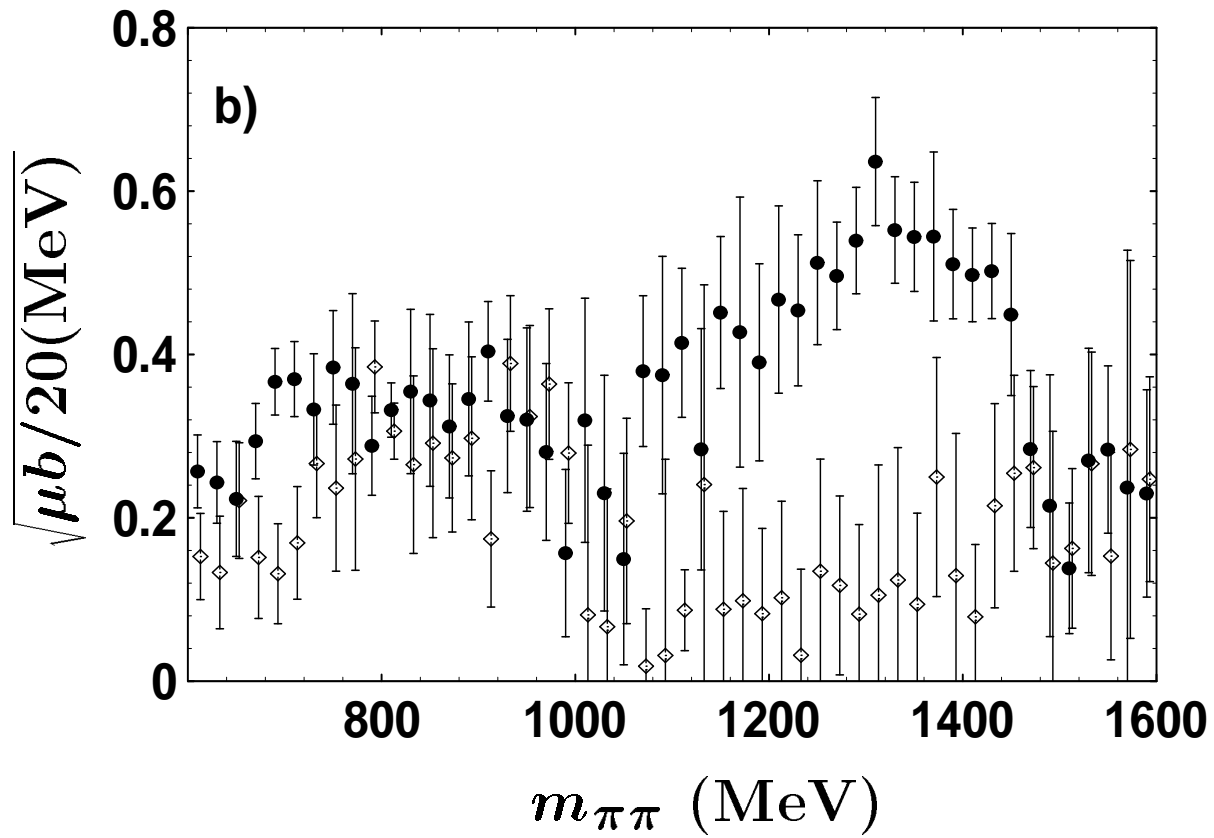
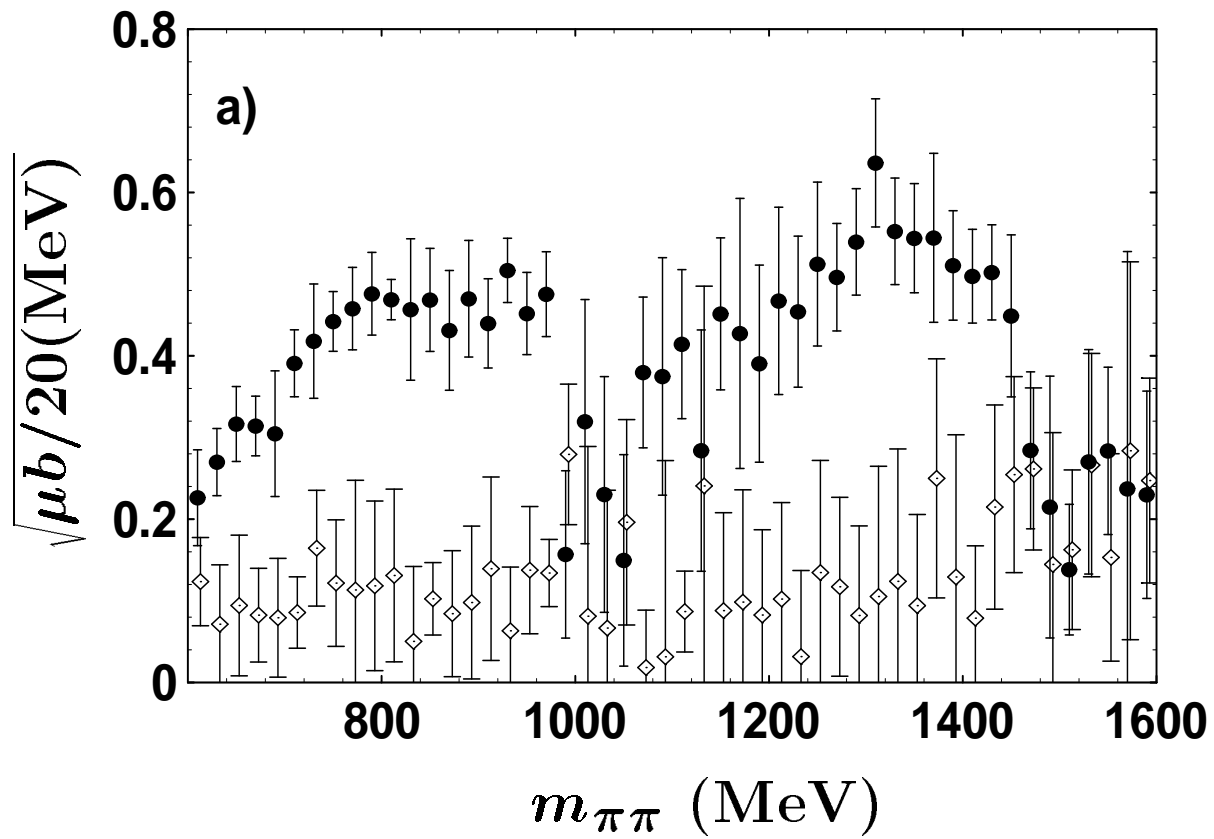


Fig. 7ab

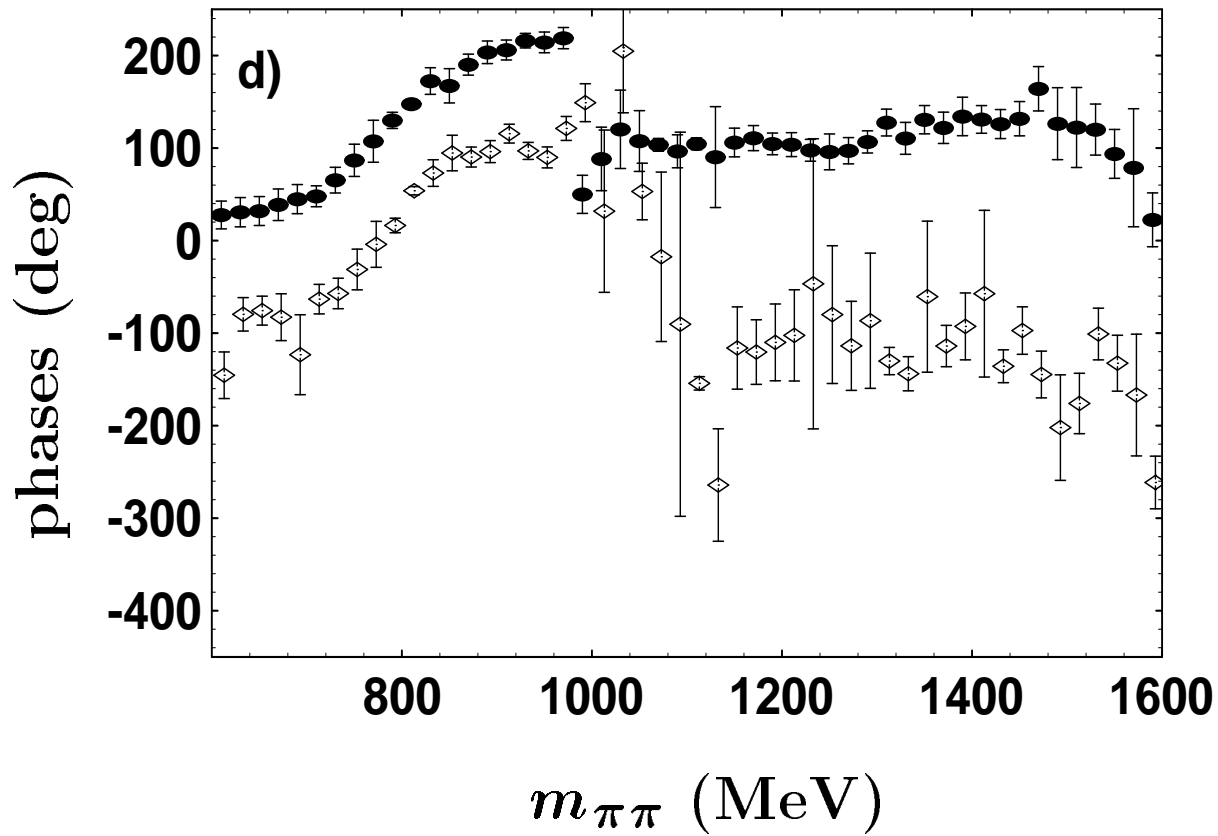
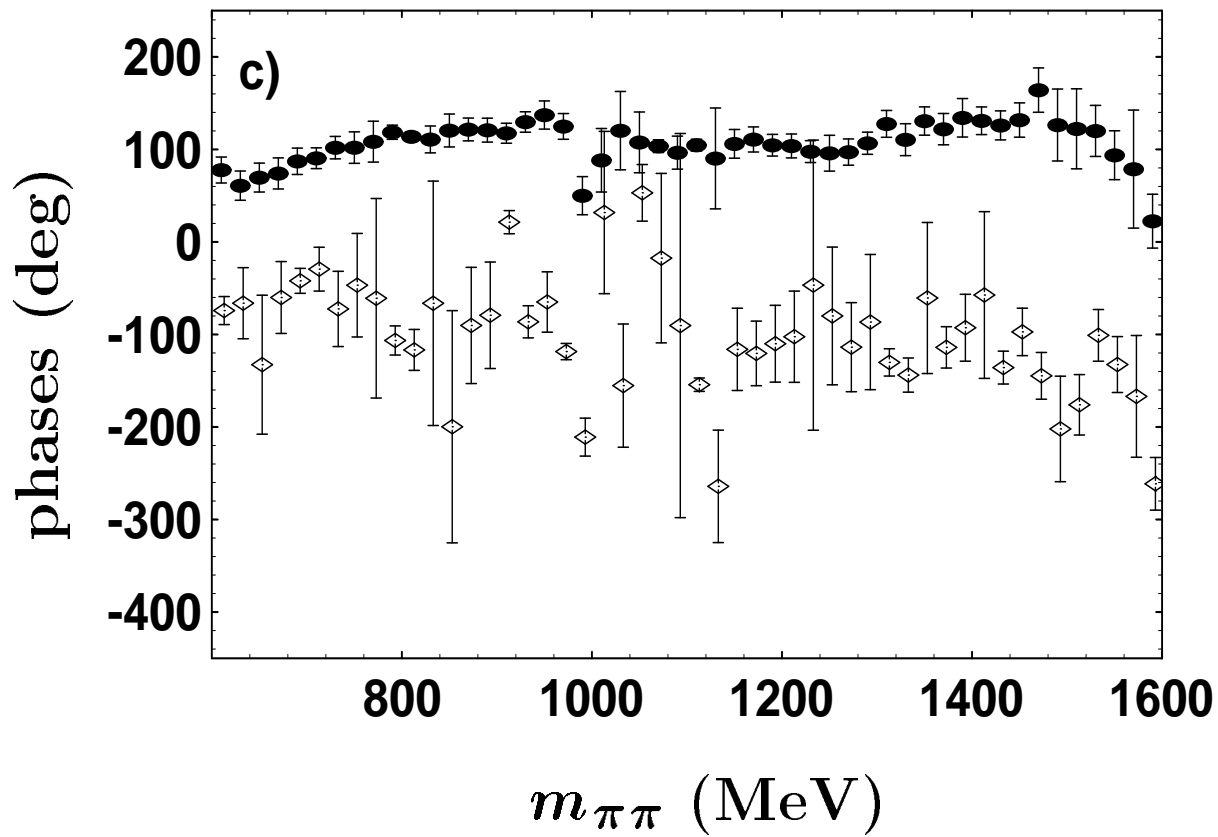


Fig. 7cd

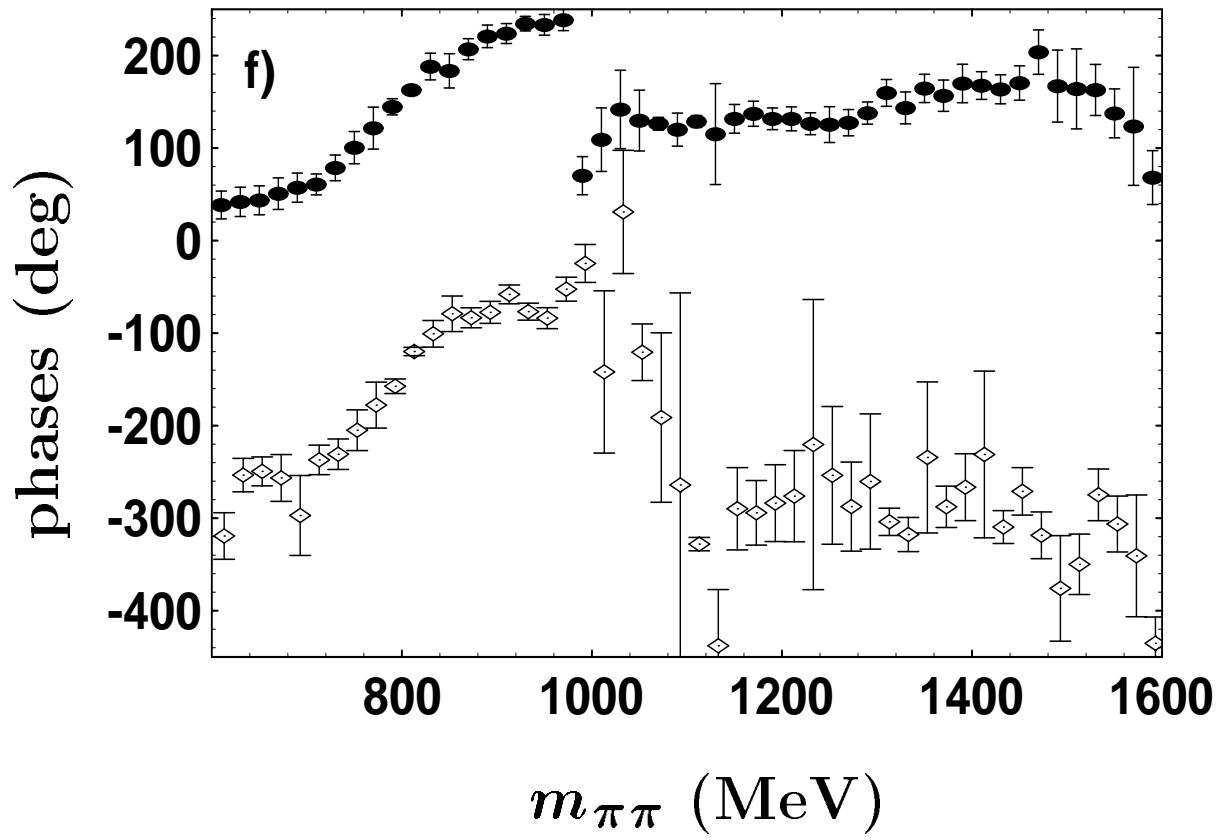
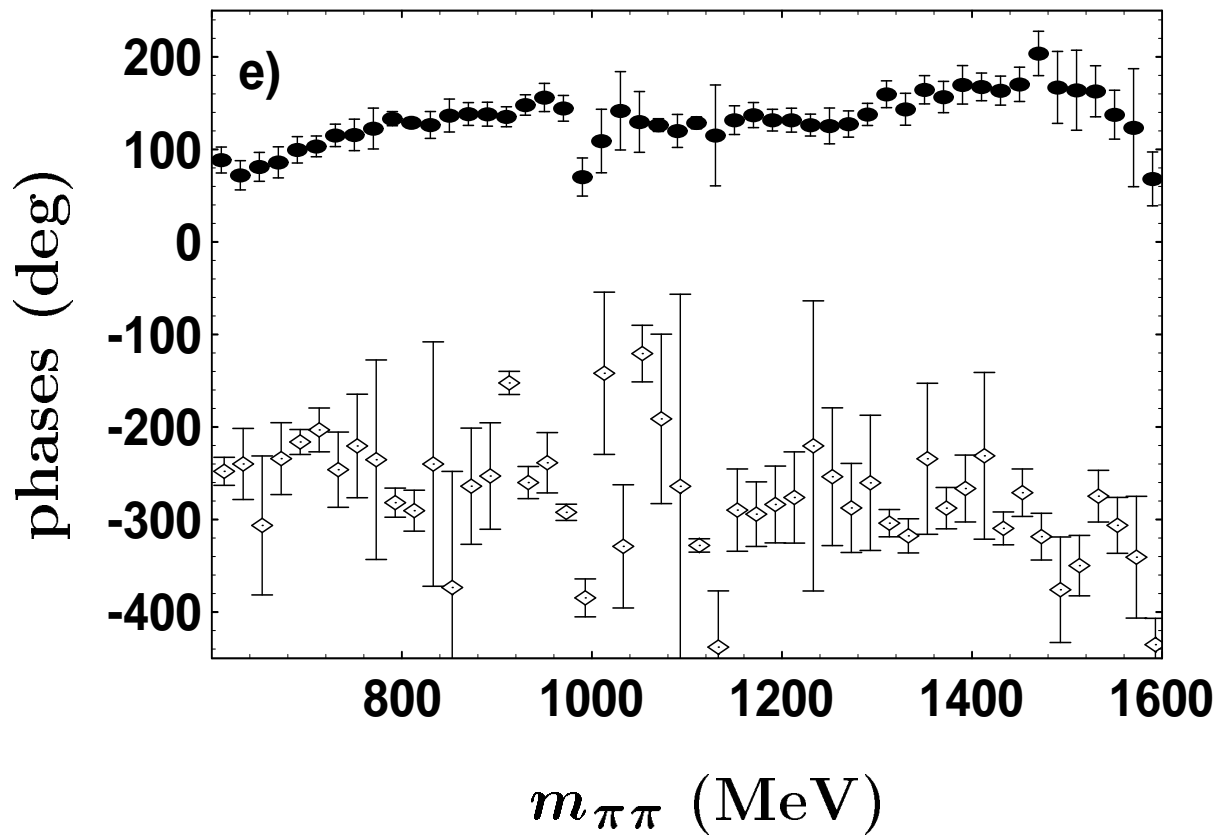


Fig. 7ef

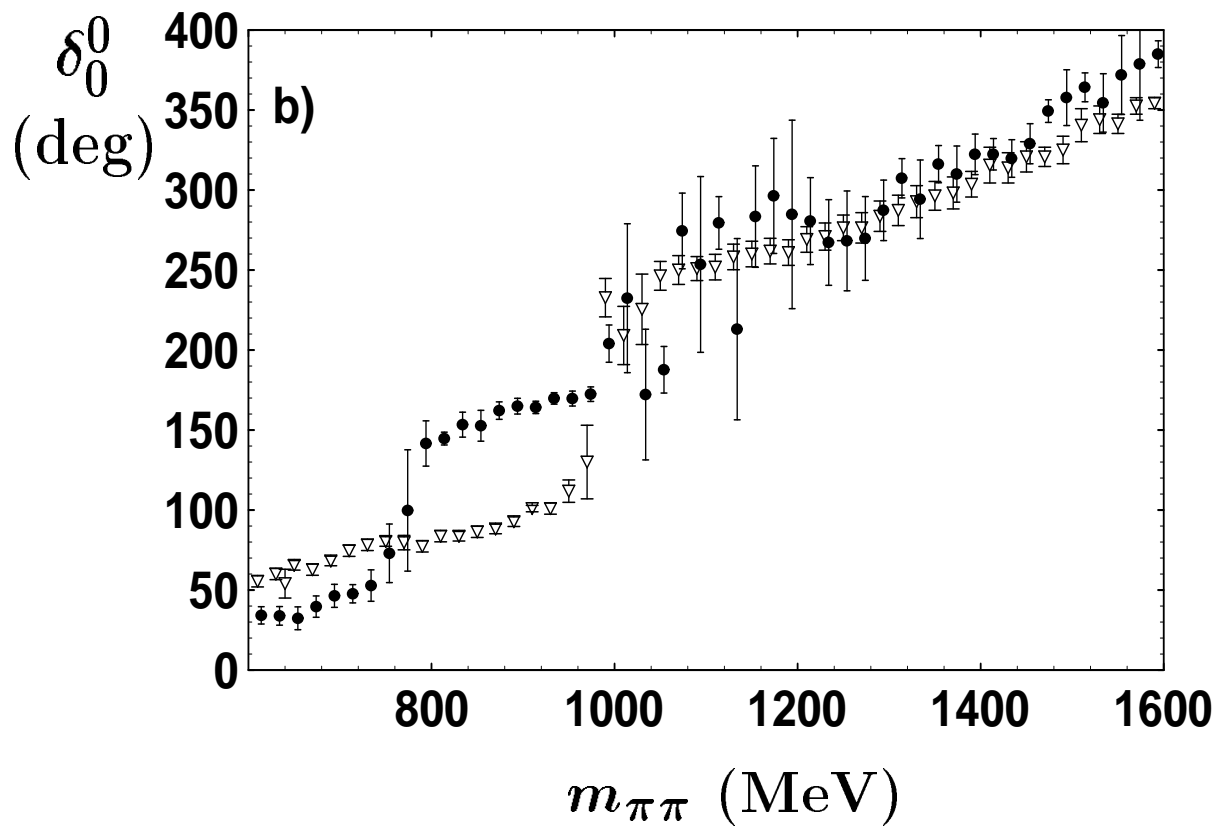
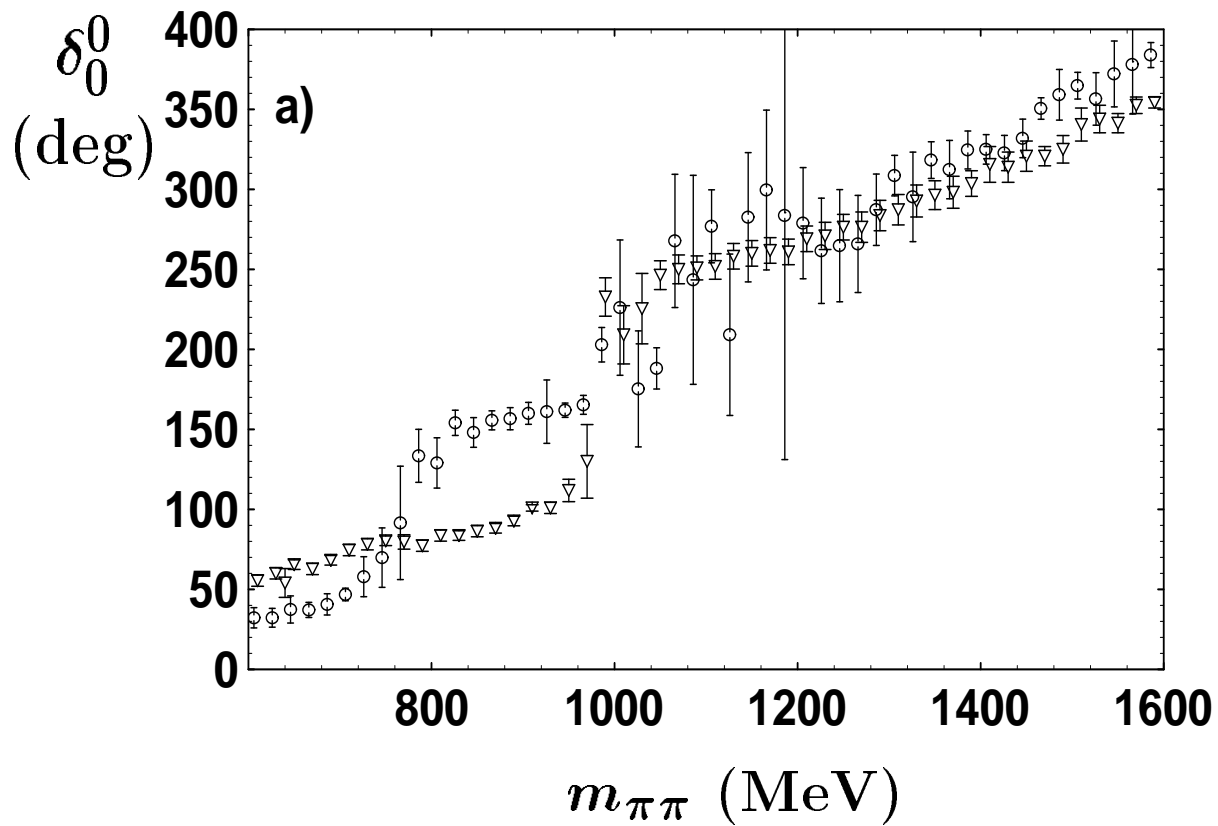


Fig. 8ab

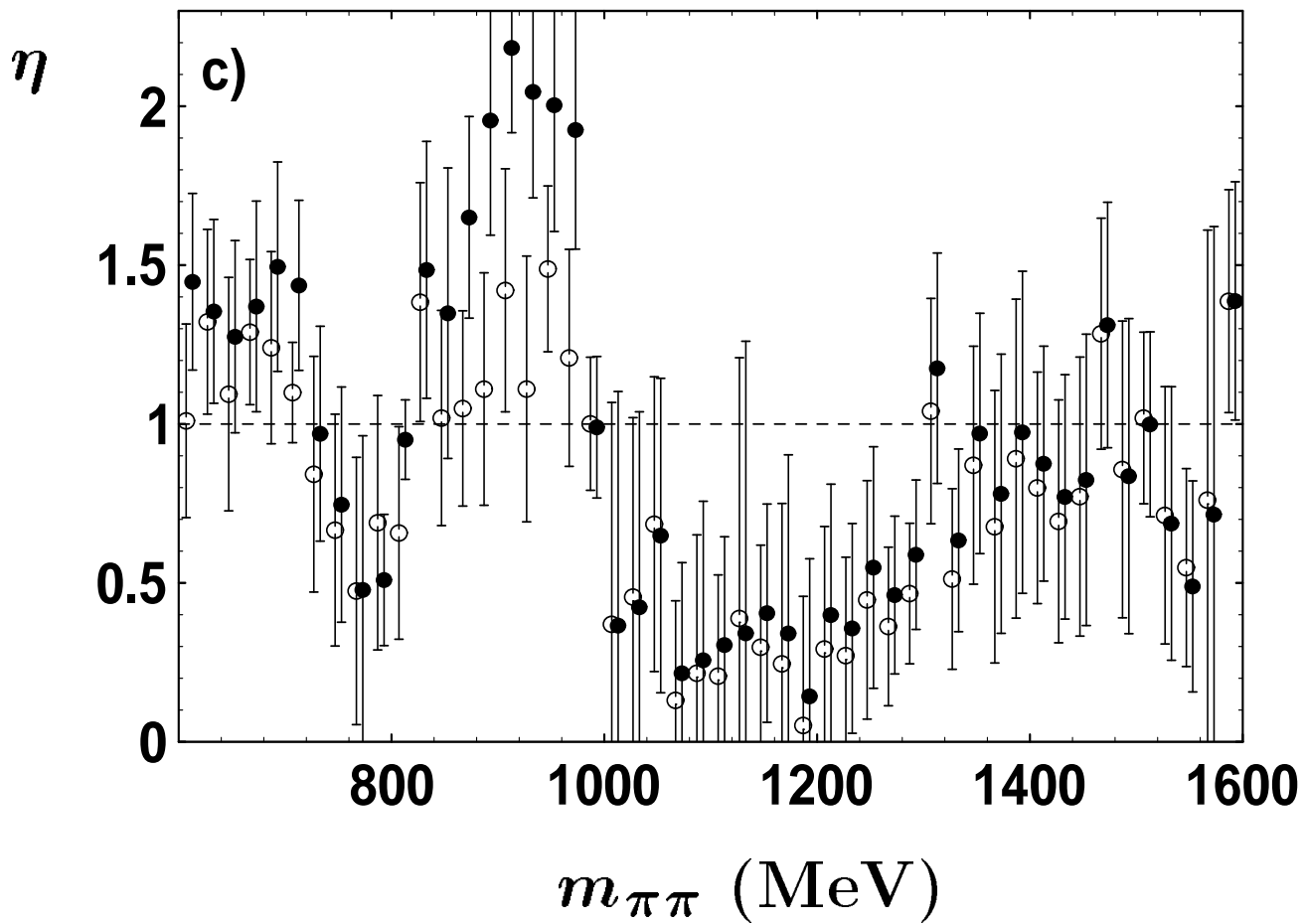


Fig. 8c

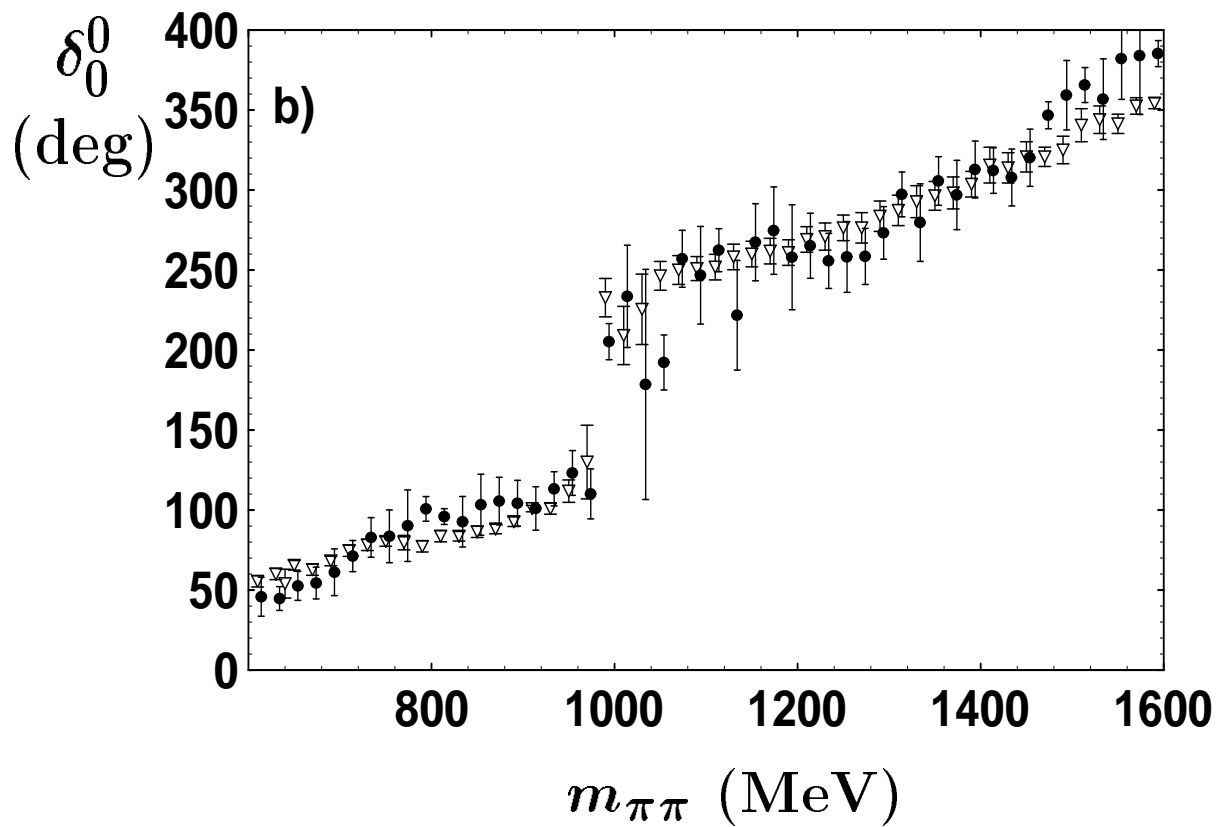
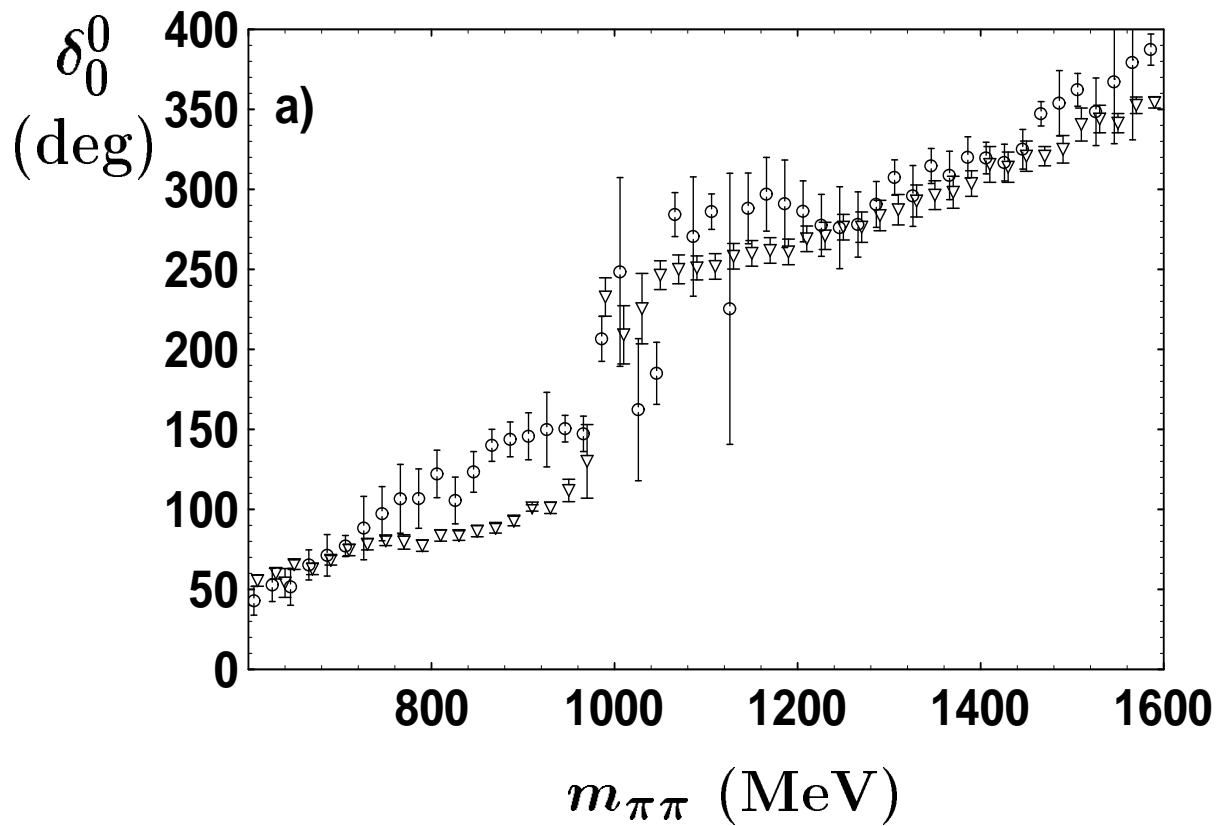


Fig. 9ab

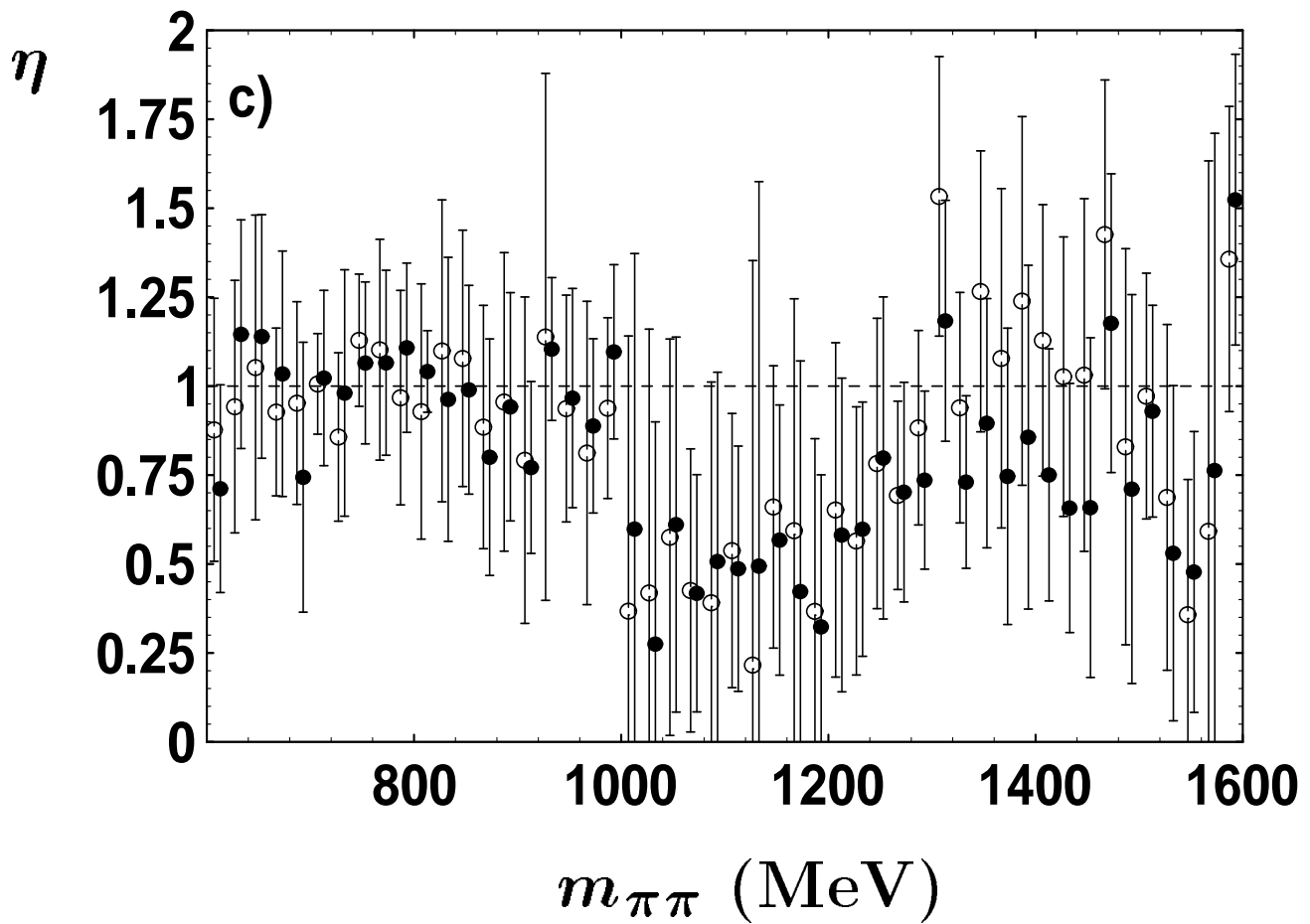


Fig. 9c